APPENDIX A

SUPPLEMENT TO CHAPTER 1

This Appendix contains detailed information about each field site including summaries of the test beds and the index properties and lab test results of the soils encountered. In addition, the lab testing and spot test measurements methods are described in detail.

A.1 MINNESOTA FIELD SITE

Phase I field testing was conducted at the MnROAD low-volume road research site in Albertville, MN, (approximately 40 miles northwest of Minneapolis/St. Paul and adjacent to Interstate 94) in July 2006. The low-volume roadway 'loop' is 3.0 km (2.5 miles) long and is comprised of many 150-m (500-ft) long pavement sections (cells). NCHRP 21-09 testing was conducted within the scope of an existing geocomposite construction project in cells 27 and 28. In addition, project 21-09 research was conducted at a nearby stockpile area where additional soil types were available and deeper test beds could be constructed.

Intelligent Compaction (IC) rollers from Ammann, Bomag and Caterpillar were used. All rollers were equipped with RTK GPS. The Ammann roller maintained a smooth drum configuration for the duration of the project. The Bomag roller was outfitted with a pad foot shell kit for the first part of the project duration. Similarly, the pad foot drum on the caterpillar roller at the beginning of the project was swapped out for a smooth drum part way through testing. The Ammann roller was equipped with the Ammann Compaction Expert (ACE) measurement system, employing the k_s MV. The Bomag roller was equipped with the Bomag Compaction Monitor (BCM) measurement system, employing the E_{vib} MV. The Caterpillar roller employed both the Geodynamik *CMV* and *MDP* MVs. The measurement systems and roller MVs are discussed in detail in Chapter 2. In addition to these measurement systems provided by the manufacturers, the research team installed independent instrumentation to measure drum and frame vibration and eccentric position on the Caterpillar roller and drum and frame vibration on the Ammann roller.

Table A.1 summarizes the 43 test beds that were constructed on cell 27/28 clay subgrade and aggregate base material, as well as in stockpile area aggregate and clayey sand soil. Table A.2 summarizes the index properties of the soils encountered.

Table A.1. Summary of MN test beds

TB	Soil	Roller(s)[1]	Remarks
MN1 MN2 MN3	Existing subgrade Existing subgrade Existing subgrade	Cat (PD) Bomag (PD) Ammann (SD)	Map starting condition of Cells 27 & 28; compare data from different rollers
MN4 MN5	Subgrade Subgrade	Bomag (PD) Cat (PD)	MV-spot test correlation; typical construction
MN6 MN7	Subgrade Subgrade	Bomag (PD) Cat (PD)	MV-spot test correlation; homogeneous construction
MN8 MN9	Subgrade Subgrade	Bomag (PD) Ammann (SD)	Map Cell 27 prior to base course; compare data from different rollers
MN10 MN11	Subgrade Subgrade	Bomag (PD) Cat (PD)	MV-spot test correlation; homogeneous soil, variable water content
MN12 MN13	Subgrade Subgrade	Bomag (PD) Cat (PD)	MV-spot test correlation; homogeneous soil, variable lift thickness
MN14	Subgrade	Cat (PD), Ammann (SD)	Test in-ground instrumentation
MN15 MN16	Subgrade Subgrade	Cat (PD) Bomag (PD)	Further investigate influence of moisture on MVs and compaction process
MN17 MN18 MN19	Subgrade Subgrade Subgrade	Ammann (SD) Ammann (SD) Ammann (SD)	MV-spot test correlation; evaluate influence of lift thickness and vibration amplitude
MN20	Subgrade	Ammann (SD)	MV-spot test correlation, static compact.
MN21 MN22	Subgrade Subgrade	Cat (SD) Bomag (SD)	MV-spot test correlation, evaluate influence of vibration amplitude
MN23	Subgrade	All (SD)	Map transition zone between Cells 27&28
MN24 MN25 MN26	Subgrade Subgrade Subgrade	Cat (SD) Bomag (SD) Ammann (SD)	MV-spot test correlation, evaluate effects of variable moisture content and vibration amplitude
MN27 MN28	Class 5 Base Class 5 Base	Bomag (SD) Bomag (SD)	Develop compaction curves for base material; MV-spot test correlation
MN29	Stockpile Area Subgrade	All (SD)	In-ground instrumentation, measurement depth studies
MN30 MN31	Subgrade Subgrade	Cat (SD) Ammann (SD)	Evaluate evolution of heterogeneity during compaction process
MN32	Subgrade	Bomag (SD)	Finish production compaction of Cell 28
MN33	Subgrade	All (SD)	Map Cell 28 prior to base course
MN34	Subgrade	Cat (SD)	Correlation between different LWDs
MN35	Class 5 Base	All (SD)	MV-spot test correlation
MN36	Class 5 Base	All (SD)	MV-spot test correlation
MN37	Class 5 Base	Bomag (SD)	MV-spot test correlation
MN38	Class 5 Base	Bomag (SD)	Map Cell 27
MN39	Class 5 Base	Cat (SD)	MV-spot test correlation
MN40	Class 5 Base	All (SD)	In-ground instrumentation, base mat'l
MN41	Class 5 Base	All (SD)	Map Cell 28
MN42 MN43	Mixed Mixed	All (SD) All (SD)	Investigate feedback control and effect of vibration amplitude on MVs

SD=smooth drum, PD=pad foot drum

Table A.2. Index properties of MN soils

Parameter	Soil						
	Borrow Subgrade	**Existing Subgrade Cells 27 and 28**	**Mixed Subgrade A**	**Mixed Subgrade B**	**Class 5 Base**	**Stockpile Area Subgrade**	**Stockpile Area Aggregate Base**
Material Description	Brown Sandy Lean Clay	Brown Sandy Lean Clay	Brown Sandy Lean Clay	Brown Sandy Lean Clay	Brown Poorly Graded Sand with Silt and Gravel	Dark Brown Clayey Sand	Gray Well Graded Gravel
Gravel Content (%) (> 4.75mm)	1	5	6	2	30	29	78
Sand Content (%) (4.75mm – 75μm)	42	39	47	37	60	35	19
Silt Content (%) (75μm – 2μm)	37	37	31	38	7	30	3[2]
Clay Content (%) (<2μm)	20	19	16	22	3	6	—
Coefficient of Uniformity (c_u)	—	—	—	—	22	—	31
Coefficient of Curvature (c_c)	—	—	—	—	0.9	—	2
Liquid Limit, LL (%)	32	26	31	32	NP	32	NP
Plasticity Index, PI	14	10	13	19	NP	14	NP
Specific Gravity, G_s	2.69[1]	2.69[1]	2.69[1]	2.69	2.71	2.69[1]	2.71[1]
AASHTO Classification	A-6 (5)	A-4(3)	A-6 (5)	A-6 (5)	A-1-b	A-6(1)	A-1-a
Unified Soil Classification (USCS)	CL	CL	CL	CL	SP-SM	SC	GW

[1]Assumed values
[2]Silt and Clay content

A.2 COLORADO FIELD SITE

Field work was carried out at the I-25 Reconstruction/Widening project near Longmont, CO (approximately 30 miles north of Denver) during August-October 2007. The construction project included considerable earthwork involving long sections (up to 1km [0.6 mi]) of both substantial cut (up to 1.25 m [4.1 ft]) and fill (up to 6+ m [20+ ft]). Two types of testing were pursued: 1) smaller scale test strips featuring detailed spot testing and correlation to roller MVs (similar to the approach used in Minnesota) and 2) larger scale production compaction allowing the various specification options to be evaluated.

IC rollers from Bomag, Caterpillar and Dynapac were used. All rollers were equipped with RTK GPS and had smooth drums for the duration of testing. Similar to testing in Minnesota, the Bomag roller was equipped with the Bomag Compaction Monitor (BCM) measurement system, employing the E_{vib} MV, and the Caterpillar roller employed both the Geodynamik *CMV* and *MDP* MVs. The Dynapac roller was equipped with the Dynapac Compaction Analyzer (DCA) employing the Geodynamik *CMV* MV. The measurement systems and roller MVs are discussed in detail in Chapter 2.

The CSM research team was onsite during parts of August, September and October 2007. Contractor delays (some due to weather) caused the extended duration of testing (originally scheduled to be two weeks). Using the Dynapac IC roller the research team compacted four lifts of the subbase material in one of the 240 m (800 ft) segments. In addition, using the Bomag IC roller the research team compacted two layers of the subbase material in one of these segments and performed one additional calibration in a different section. Dynapac CMV or Bomag E_{vib} and spot test (LWD and nuclear gage) data were collected during compaction. The objective of this work was to evaluate the European specification options and to continue to develop new recommendation for specification options in the U.S.

The ISU research team conducted field testing at the CO project site from August 20, 2007 to August 29, 2007. Subgrade work consisted of three 15 m (50 ft) long sections with variable moisture conditions. One subgrade section (section 4) was left un-compacted with relatively wet moisture conditions prior to placing subsequent subbase/base layers. The remaining three subgrade sections (sections 1 to 3) were compacted using all three rollers (Bomag, CAT, Dynapac) in four lanes in conjunction with in-situ spot test measurements (nuclear gauge, LWD, DCP, and plate load test). Two 30 cm (1 ft) thick subbase layers and one 15 cm (0.5 ft) thick base layer were placed over the subgrade and compacted using the three rollers.

Table A.3 summarizes the 43 test beds that were constructed on existing clay subgrade, and aggregate subbase and base course materials. Table A.4 summarizes the index properties of the soils encountered.

Table A.3. Summary of CO test beds

Test Bed	Soil	Roller	Remarks
CO1	Subgrade	Bomag	MV-spot test correlations, variable moisture (Lane 1)
CO2	Subgrade	Bomag	MV-spot test correlations, variable moisture (Lane 2)
CO3	Subgrade	Dynapac	MV-spot test correlations, variable moisture (Lane 3)
CO4	Subgrade	CAT	MV-spot test correlations, variable moisture (Lane 4)
CO5	Subgrade	ALL	Subgrade map (4 lanes using all three rollers)
CO6	Subbase	Bomag	MV-spot test correlations (layer on top of TB 1, Lane 1)
CO7	Subbase	Bomag	MV-spot test correlations (layer on top of TB 2, Lane 2)
CO8	Subbase	Dynapac	MV-spot test correlations (layer on top of TB 3, Lane 3)
CO9	Subbase	CAT	MV-spot test correlations (layer on top of TB 4, Lane 4)
CO10	Subbase	ALL	Subbase layer 1 map (4 lanes)
CO11	Subbase	Bomag	MV-spot test correlations (layer on top of TB 6, Lane 1)
CO12	Subbase	Bomag	MV-spot test correlations (layer on top of TB 7, Lane 2)
CO13	Subbase	Dynapac	MV-spot test correlations (layer on top of TB 8, Lane 3)
CO14	Subbase	Dynapac	MV-spot test correlations (layer on top of TB 9, Lane 4)
CO15	Subbase	ALL	Subbase layer 2 map (4 lanes)
CO16	Base	Bomag	MV-spot test correlations (layer on top of TB 11, Lane 1)
CO17	Base	Bomag	MV-spot test correlations (layer on top of TB 12, Lane 2)
CO18	Base	Dynapac	MV-spot test correlations (layer on top of TB 13, Lane 3)
CO19	Base	Dynapac	Basecourse layer map (4 lanes; Lane 4 uncompacted)
CO20	Base	Bomag, CAT	Basecourse layer map (4 lanes)
CO21	Subgrade	ALL	Repeatability study using all three rollers
CO22	Subbase	Bomag	How to best compact study 1 (2 lanes)
CO23	Subbase	Bomag	How to best compact study 2 (4 lanes)
CO24	Subbase	Bomag	Influence of speed on Evib
CO25	Subbase	Dynapac	CMV repeatability study
CO26	Subgrade	Dynapac	Production Area 1, subgrade maps
CO27	Subbase	Dynapac	Production Area 1, layer 1 calibration and production
CO28	Subbase	Dynapac	Production Area 1, layer 2 calibration and production
CO29	Subgrade	Bomag	Production Area 2, subgrade map
CO30	Subbase	NA	LWD sand study
CO31	Subbase	Bomag	Production Area 1, layer 3 calibration only
CO32	Subbase	Dynapac	Production Area 1, layer 3 calibration and production
CO33	Subbase	Dynapac	Dependence of CMV on speed and amplitude (layer 3)
CO34	Subbase	Dynapac	Production Area 1, layer 4 calibration and production
CO35	Subbase	Dynapac	Dependence of CMV on speed and amplitude (layer 4)
CO36	Subbase	Dynapac	Dependence of CMV on speed and driving direction (layer 4)

Table A.3. Summary of CO test beds, Continued

Test Bed	Soil	Roller	Remarks
CO37	Subbase	Dynapac	Soft spot test (layer 4)
CO38	Subgrade	Bomag	Production Area 3, subgrade map
CO39	Subbase	Bomag	Production Area 3, layer 1 calibration and production
CO40	Subbase	Bomag	Dependence of Evib on vibration amplitude
CO41	Subbase	Bomag	Evib repeatability and forward-reverse repeatability
CO42	Subbase	Bomag	Dependence of Evib on speed
CO43	Subbase	Bomag	Production Area 3, layer 3 calibration and production

Table A.4: Index properties of CO soils

Parameter	Soil				
	Subgrade			Subbase	Base
Material Description	Sandy lean clay	Clayey to silty sand	Sandy lean clay	Well graded gravel to silty gravel with sand	Poorly graded sand with silt
Maximum dry unit weight (kN/m^3) and optimum moisture content (%)					
Standard Proctor	18.74 (11.8)	18.54 (14.2)	16.48 (17.8)	—	21.25 (8.0)
Modified Proctor	19.82 (9.8)	19.48 (10.2)	18.54 (10.5)	—	21.54 (7.1)
Gravel Content (%) (> 4.75mm)	1	11	1	66	44
Sand Content (%) (4.75mm – 75μm)	31	47	30	28	49
Silt Content (%) (75μm – 2μm)	39	28	37	3	4
Clay Content (%) (< 2μm)	29	14	22	3	3
Coefficient of Uniformity (c_u)	—	69.4	—	150.7	32.3
Coefficient of Curvature (c_c)	—	5.0	—	2.0	0.3
Liquid Limit, LL (%)	30	30	27	NP	NP
Plasticity Index, PI	13	7	10	NP	NP
AASHTO	A-6(7)	A-4	A-4(3)	A-1-a	A-1-a
USCS	CL	SC-SM	CL	GW-GM	SP-SM
G_s	2.65*	2.57	2.74	2.65	2.65

* Assumed

A.3 MARYLAND FIELD SITE

Field testing was conducted from October 22nd through November 9th, 2007 at the I-70 interchange and accompanying roads construction project in Frederick, Maryland. The site involved 1-2 m (3-6 ft) fill sections (silty clay/clayey silt) in numerous locations and 30 cm (12 in) of aggregate base course. The project also included compaction of pond basins with 30 cm (12 in) of granular material.

Heavy rains during the week of October 22nd forced modifications to the correlation study and production compaction research plans. Though large production areas of subgrade and base material placement and compaction were planned by the contractor for this time frame, no production compaction took place during the research team's time on site due to the weather and contractor delays. To evaluate the implementation of specification options during production compaction, researchers must rely on contractor production and the cooperation of weather. This is an unavoidable risk, and given the existing scheduling challenges (two universities, 3 roller manufacturers, the construction site personnel, open houses), these time frames can not be rescheduled at the last minute. With that said, the research team was able to modify the work plan to accommodate the site conditions and conduct valuable investigations.

IC rollers from Bomag (smooth drum), Dynapac (smooth drum and pad foot via shell kit) and Sakai (smooth drum) were used. All rollers were equipped with RTK GPS. The Bomag roller was equipped with the Bomag Compaction Monitor (BCM) measurement system, employing the E_{vib} MV. The Dynapac roller was equipped with the Dynapac Compaction Analyzer (DCA) employing the Geodynamik *CMV* MV. The Sakai roller was equipped with a prototype version of the Compaction Information System (CIS) employing the *CCV* MV. The measurement systems and roller MVs are discussed in detail in Chapter 2.

ISU field testing involved preparation of one subgrade test bed for repeatability testing and fourteen test beds comprised of a subgrade layer and two overlying aggregate base layers. The test bed area for ISU testing consisted of a 60 m (200 ft) x 15 m (50 ft) section with variable underlying conditions consisting of subgrade soil and concentrations of fractured rock. The subgrade layer was scarified several times over a two day period with a motor grader in an effort to aerate and dry the soil and to provide a relatively uniform uncompacted condition. The scarification depth was approximately 25 cm (10 in). In-situ moisture content measurements showed that the subgrade was generally wet of optimum moisture content based on standard Proctor results. Two base layers of approximately 18-20 cm (7-8 in) loose thickness each were placed over the subgrade layer and compacted using three rollers in four or five different lanes.

The test objectives were to (1) Develop linear and multiple regression relationships between roller MVs and in-situ soil properties (soil moisture, dry unit weight, strength, stiffness, and pad foot penetration depth) for the subgrade soil and base layers; (2) Understand the influence of speed and amplitude on the compaction process and roller MVs; and (3) Evaluate the benefits of feedback control.

The CSM research team performed several roller MV repeatability studies and investigations of the influence of soil heterogeneity on roller MVs. For these studies, all smooth drum rollers were employed. Spot testing included Zorn LWD and moisture/density (via nuclear gage performed by Maryland DOT personnel). In total, 5 subgrade and 2 base course test beds were completed. In addition, due to the weather-induced modifications required, we expanded the scope of in ground instrumentation in a trench type test bed. Test objectives included (1) gathering in-situ stress strain data from a layered system comprised of base course (stiff material) atop soft subgrade material (clay wet of optimum moisture), (2) gathering in-situ stress strain data from a layered system comprised of base course (stiff material) atop a stiffer subgrade material (clay near optimum moisture), (3) gathering roller MV data during layer build-up to further the measurement depth analysis initiated in Minnesota. This test bed was conducted over eight days.

Table A.5 summarizes the 23 test beds that were constructed on subgrade, and aggregate subbase and base course materials in Maryland. Table A.6 summarizes the index properties of the soils encountered.

Table A.5. Summary of MD test beds

Test Bed	Soil	Roller(s)	Remarks
MD1	Subgrade	Dynapac (PD), Bomag (SD), Sakai (SD)	Roller MV repeatability
MD2-5	Subgrade	Dynapac (PD), Bomag (SD), Sakai (SD)	MV-Spot Test Correlations
MD6-10	Base	All (SD)	MV-Spot Test Correlations
MD11-15	Base	All (SD)	MV-Spot Test Correlations
MD16	Subgrade	Bomag (SD)	Local Variability
MD17	Subgrade	Dynapac (PD)	Roller MV repeatability
MD18	Subgrade	Bomag (SD)	Local Variability
MD19	Subgrade, Subbase	All (SD)	In-ground instrumentation, measurement depth
MD20	Subgrade	All (SD)	Roller MV repeatability, local variability
MD21	Subgrade	Bomag (SD)	Roller MV position reporting errors
MD22	Base	All (SD)	Roller MV repeatability, local variability
MD23	Subgrade	All (SD)	Roller MV repeatability, local variability

Table A.6. Summary of soil index properties from Maryland project

Parameter	Soil			
	Subgrade	**Subgrade**	**Subbase**	**Base**
Description	Silty sand	Clayey Sand	Silty sand	Poorly graded sand with silt and gravel
Maximum dry unit weight (kN/m^3) and optimum moisture content (%)				
Standard Proctor	18.93 (11.9)			22.48 (5.9)
Modified Proctor	20.09 (9.7)			22.97 (5.2)
Gravel Content (%) (> 4.75mm)	6	8	4	42
Sand Content (%) (4.75mm – 75μm)	65	43	81	46
Silt Content (%) (75μm – 2μm)	10	25	12	12
Clay Content (%) (< 2μm)	19	18	3	0
Coefficient of Uniformity (c_u)	—		66	—
Coefficient of Curvature (c_c)	—		4	—
Liquid Limit, LL (%)	22	30	—	NP
Plasticity Index, PI	NP	9	—	NP
AASHTO	A-2-4	A-4(1)	A-1-b	A-1-a
USCS	SM	SC	SM	SP-SM
G_s (assumed)	2.65	2.65	2.70	2.70

A.4 FLORIDA FIELD SITE

Field testing was conducted from April 4-24, 2008 at the Branan Field Chaffe/I-10 Interchange and accompanying divided highway project near Jacksonville, FL. In total, 26 test beds were constructed to allow the evaluation of three different materials: (1) fine sand subgrade; (2) ash stabilized fine sand subgrade; and (3) limerock base material. The rollers used for testing included Case/Ammann smooth drum, Dynapac smooth drum and Sakai smooth drum. The Sakai roller was instrumented to measure drum and frame acceleration and eccentric position by the CSM research team, allowing independent calculation of the various MVs. All rollers were equipped with RTK GPS. The CSM research team conducted field testing from April 4-17 followed by the ISU research team which conducted testing from April 16-24. This staggered approach was used to allow both teams to use the rollers and to minimize the daily impact on the contractor.

While on site, the CSM research team performed several roller MV repeatability studies, investigations of the influence of soil heterogeneity and anisotropy on roller MVs and studies to help determine how to best compact soil using IC rollers. For these studies, all smooth drum rollers were employed. Spot testing included Zorn LWD, Dynatest LWD, Dynatest FWD (performed by FDOT personnel) surface seismic and moisture/density (via nuclear gage performed by FDOT personnel). In total, four subgrade, nine stabilized subgrade and five base course test beds were completed. In-ground instrumentation was employed in a large, layered test bed. Instrumentation was installed in embankment and stabilized subgrade (atop the embankment) layers and subsequently, four 15 cm (6 in) layers of base material were placed and compacted. Instrumented test bed objectives included: (1) gathering three dimensional in-situ stress-strain data from a layered system consisting of embankment, stabilized subgrade and base course material, (2) collecting data to determine how the stress-strain field varies across the width of the drum, (3) collecting data to determine how forward velocity, driving direction and excitation amplitude and frequency affect the stress-strain field and roller MVs and (4) collecting roller and spot test data during the compaction of thin, stiff layers atop softer subgrade material.

The ISU research team focused their efforts on the evaluation of specification options. Test bed construction involved compacting and testing calibration test strips to develop target roller MVs in relationship with target QA values, and compacting and testing production areas. Testing focused on developing datasets for evaluating proposed specification options. Samples of embankment subgrade and aggregate base material were reconstituted for laboratory resilient modulus (M_r) testing. Results were used to develop empirical relationships between roller MVs and laboratory M_r for specification option 3c. A total of seven test beds were constructed. Of these, four test beds consisted of aggregate base material (15-30 cm [6-12 in] thick) over compacted stabilized subgrade, two test beds consisted of embankment subgrade materials, and one test bed consisted of stabilized embankment subgrade material. In-situ tests included static plate load, lightweight deflectometer, nuclear moisture-density gage, and dynamic cone penetrometer tests.

Table A.7 summarizes the 26 test beds that were constructed on subgrade, stabilized subgrade and aggregate base course materials in Florida. Table A.8 summarizes the index properties of the soils encountered.

Table A.7. Summary of FL test beds

Test Bed	Soil	Roller(s)	Remarks
FL1	Subgrade	Sakai	In-ground instrumentation - Compacting & mapping of subsurface, & full testing of subgrade layer
FL2	Stab. Sub.	Sakai	In-ground instrumentation - Full testing of stabilized subgrade layer
FL3	Base	Sakai	In-ground instrumentation - Full testing of base layer 1
FL4	Base	All	In-ground instrumentation - Full testing of base layer 2 (incl. FWD)
FL5	Base	Sakai	In-ground instrumentation - Full testing of base layer 3
FL6	Base	All	In-ground instrumentation - Full testing of base layer 4 (incl. FWD)
FL7	Stab. Sub.	Sakai	Heterogeneity
FL8	Stab. Sub.	Sakai	Heterogeneity, Low amp, High amp, multiple frequencies on main road
FL9	Stab. Sub.	Sakai	Heterogeneity, lower area, low amp, several frequencies
FL10	Subgrade	Sakai	How to best compact - confinement study 1 (on TB1, subsurface)
FL11	Subgrade	Sakai	How to best compact - amplitude variation (on TB1, subgrade layer)
FL12	Stab. Sub.	Sakai	Measurement error & repeatability
FL13	Stab. Sub.	Sakai	Same as TB8 but on lower area
FL14	Stab. Sub.	Sakai	Heterogeneity 4 lane study on lower area
FL15	Stab. Sub.	Sakai	Calibration on FL2 (In-ground TB - stab. subgrade), Zorn LWD & Nuke
FL16	Subgrade	Sakai	Anisotropy
FL17	Base	Sakai	Calibration on FL4 (In-ground TB - 2nd layer of base), Zorn LWD
FL18	Stab. Sub.	All	Position error/repeatability (wood tests)
FL19	Stab. Sub.	Dynapac	MV-Spot Test correlation
FL20	Base	Case	MV-Spot Test correlation
FL21	Base	Case	MV-Spot Test correlation
FL22	Base	Case, Dynapac	MV-Spot Test correlation
FL23	Subgrade	Case, Dynapac	MV-Spot Test correlation
FL24	Stab. Sub.	Case, Dynapac	MV-Spot Test correlation
FL25	Stab. Sub	Case, Dynapac	Roller MV repeatability
FL26	Subgrade	Case, Dynapac	MV-Spot Test correlation

Table A.8. Summary of soil index properties from Florida project

Parameter	Soil					
	Base		Stabilized Subgrade		Subgrade	
Material Description	Silty sand with gravel	Silty sand with gravel	Poorly graded sand to silty sand	Silty sand	Silty sand	Poorly graded sand to silty sand
Maximum dry unit weight (kN/m^3) and optimum moisture content (%)						
Standard Proctor	17.93 (13.1)	18.38 (14.2)	15.9 (8.3)	16.12 (18.0)	16.4 (17.3)	15.6 (12.5)
Modified Proctor	18.22 (11.5)	19.01 (12.2)	16.3 (8.3)	17.28 (15.8)	17.5 (15.0)	15.8 (10.9)
Gravel Content (%) (> 4.75mm)	30	28	1	6	1	0
Sand Content (%) (4.75mm – 75µm)	49	48	94	81	85	94
Silt Content (%) (75µm – 2µm)	16	17	1	10	11	2
Clay Content (%) (< 2µm)	5	7	4	3	3	4
Coefficient of Uniformity (c_u)	283.9	333.4	2.4	5.9	4.8	2.4
Coefficient of Curvature (c_c)	2.3	3.6	1.0	2.4	1.6	1.1
Liquid Limit, LL (%)	NP	NP	NP	NP	NP	NP
Plasticity Index, PI	NP	NP	NP	NP	NP	NP
AASHTO	A-1-b	A-1-b	A-3	A-2-4	A-2-4	A-3
USCS	SM	SM	SP-SM	SM	SM	SP-SM
G_s (assumed)	2.65	2.65	2.65	2.65	2.65	2.65

A.5 NORTH CAROLINA FIELD SITE

Field testing was conducted from May 19 – June 7, 2008 at the NC311/I-85 divided highway project near High Point, NC (5 miles south of Greensboro). This 7-mile long project was a new construction of divided Interstate highway. Earthwork sections were 12-15 m (40-50 ft) wide. In total, 36 test beds were created with cohesive and granular subgrade materials as well as aggregate base material. The ISU research team conducted testing from May 19 - May 27, followed by CSM testing from May 27 - June 7. As with testing in Florida, this staggered approach was used to allow both teams to use the rollers and to minimize the daily impact on the contractor.

The rollers used for testing included Bomag smooth drum, Case/Ammann smooth drum, Sakai smooth drum and Caterpillar pad foot. The CSM research team installed independent instrumentation on the Sakai roller to measure drum and frame acceleration and eccentric position and on the Bomag roller to measure drum acceleration. All rollers were equipped with RTK GPS.

The ISU research team was on site from May 19 - 27. A detailed work plan was developed for evaluating specification options with three test beds on embankment subgrade material, two test beds on stabilized subgrade, and three test beds on aggregate base material. Due to weather delays and some site restrictions, the field testing focused on three test beds with subgrade material and one test bed with aggregate base material. In-place embankment subgrade and aggregate base layers were scarified to a depth of about 15-20 cm (6-8 in) in preparation of the test beds.

Samples of embankment subgrade and aggregate base material were reconstituted for laboratory M_r testing. Results were used to develop empirical relationships between roller MVs and laboratory M_r for option 3c. Test bed construction involved compacting and testing calibration test strips for developing target MVs (in relationship with QA target values) and compacting and testing production areas. In-situ tests included static plate load, lightweight deflectometer, nuclear moisture-density gauge, and dynamic cone penetrometer tests. Results are expected to help populate correlations between roller MVs and in-situ spot tests for the specification options. The Caterpillar pad foot roller equipped with the machine drive power (*MDP*) based *CCV* measurement system was used to compact embankment subgrade material in an area with variable slope conditions. The *CCV* data indicated that the measurements were sensitive to slope angle, i.e., high *CCV*-values uphill and low *CCV*-values downhill. The results are being analyzed by the manufacturer to re-evaluate calibration input parameters. Since the *CCV* data did not appear reliable, additional spot test measurements were not performed.

The CSM research team performed several studies to help determine how to best compact soil using IC rollers. In addition, investigations of the influence of soil heterogeneity and anisotropy on roller MVs and production scale test beds to evaluate the European specification options were also performed. For these studies, all smooth drum rollers were employed. Spot testing included Zorn LWD, Prima LWD, Dynatest FWD (performed by NCDOT personnel) surface seismic and moisture/density (via nuclear gage and the balloon method, both performed by NCDOT personnel). In total, 18 granular subgrade and 14 base course material test beds were completed. In addition, in-ground instrumentation was employed in a layered test bed similar to that constructed in Florida. Instrumentation was installed in subgrade material and subsequently a 15 cm (6 in) layer of base material was placed and compacted. After all testing on this layer was complete, this 15 cm (6 in) layer was scarified and an additional 15 cm (6 in) of base material was placed. Instrumentation was then installed in this now 30 cm (12 in) thick layer. The layer was compacted and tested. This lift sequence was repeated atop the first 30 cm (12 in) of base material, for a total of 60 cm (24 in) of base material atop the subgrade (no further instrumentation was installed in the third or fourth layers). This testing occurred over 5 days. Instrumented test bed objectives included: (1) gathering three dimensional in-situ stress-strain data from a layered system consisting of subgrade and base course material, (2) collecting data to determine how the stress-strain field varies across the width of the drum, (3) collecting data to determine how forward velocity, driving direction and excitation amplitude and frequency affect the stress-strain field and roller MVs, (4) collecting roller and spot test data during the compaction of thin, stiff layers atop softer subgrade material and (5) to determine the

effects of stiff layer thickness on material compactability, roller-induced stress-strain field and the roller's ability to sense stiff layers atop softer layers.

Table A.9 summarizes the 26 test beds that were constructed on subgrade and aggregate base course materials in North Carolina. Table A.10 summarizes the index properties of the soils encountered.

Table A.9. Summary of NC test beds

Test Bed	Soil	Roller(s)	Remarks
NC1	Subgrade	Bomag	MV-Spot Test correlation
NC2	Subgrade	Bomag, Case	MV-Spot Test correlation
NC3	Subgrade	Cat (PD)	MV-Spot Test correlation
NC4	Base	Bomag, Case	MV-Spot Test correlation
NC5	Subgrade	Sakai	Spot test-MV correlation study
NC6	Subgrade	Sakai, Bomag	In-ground sensors TB – subgrade layer
NC7	Base	Bomag	In-ground sensors TB – 6" base layer
NC8	Base	Sakai, Bomag	In-ground sensors TB – 12" base layer
NC9	Base	Bomag	In-ground sensors TB – 6" base layer
NC10	Base	Sakai, Bomag	In-ground sensors TB – 12" base layer
NC11	Subgrade	Sakai	MV dependence on Operating parameters
NC12	Subgrade	Sakai	Influence of amplitude on compaction
NC13	Subgrade	Sakai	Influence of confinement on compaction
NC14	Subgrade	Sakai	Influence of confinement on compaction
NC15	Subgrade	Sakai	Influence of amplitude on compaction
NC16	Subgrade	Sakai	Influence of speed on compaction
NC17	Subgrade	Sakai, Bomag	Local variability
NC18	Subgrade	Sakai, Bomag	Local variability
NC19	Base	Bomag	Spot test-MV correlation
NC20	Subgrade	Sakai, Case	Subgrade calibration area
NC21	Base	Sakai, Bomag	Base *Evaluation Section (Layer 1)*
NC22	Base	Sakai, Bomag	Base *Evaluation Section* (Layer 2)
NC23	Subgrade	Sakai, Bomag	Subgrade Evaluation Section
NC24	Subgrade	Sakai	Local variability study
NC25	Base	Sakai, Bomag	Base *Evaluation Section*
NC26	Base	Case	Feedback control study
NC27	Subgrade	Sakai, Case	Local variability study
NC28	Subgrade	Bomag	Local variability study
NC29	Subgrade	Sakai	
NC30	Both	Sakai	Subgrade & Base *Evaluation Section* proof roll
NC31	Subgrade	Sakai, Bomag	Subgrade *Evaluation Section* proof roll
NC32	Subgrade	Sakai, Case	Local variability study

Table A.9. Summary of NC test beds, Continued

Test Bed	Soil	Roller(s)	Remarks
NC33	Subgrade	Case	MV dependence on amplitude
NC34	Subgrade	Case	Influence of feedback control
NC35	Subgrade	Bomag	Influence of feedback control
NC36	Subgrade	Sakai	Stationary vibration

Table A.10. Summary of soil index properties from North Carolina project

Parameter	Soil		
	Subgrade		Base
Material Description	Silty sand	Silty sand	Poorly graded sand to silty sand with gravel
Maximum dry unit weight (kN/m^3) and optimum moisture content (%)			
Standard Proctor	19.13 (11.0)	17.39 (12.8)	21.21 (6.3)
Modified Proctor	20.39 (8.1)	19.01 (11.2)	21.85 (5.9)
Gravel Content (%) (> 4.75mm)	5	1	42
Sand Content (%) (4.75mm – 75μm)	69	61	47
Silt Content (%) (75μm – 2μm)	11	31	9
Clay Content (%) (< 2μm)	15	7	2
Coefficient of Uniformity (c_u)	—	90.5	85.4
Coefficient of Curvature (c_c)	—	1.9	0.8
Liquid Limit, LL (%)	19.5	28.4	NP
Plasticity Index, PI	NP	NP	NP
AASHTO	A-2-4	A-4	A-1-a
USCS	SM	SM	SP-SM
G_s (assumed)	2.65	2.65	2.65

A.6 LAB TESTING METHODS

Laboratory testing involved determining soil index properties, moisture-density relationships, resilient modulus, and shear strength properties. A brief overview of the objectives, laboratory testing methods, and discussion of the test results and findings is presented in this section.

A.6.1 Soil Index Properties

Soil index properties were determining using following ASTM standard test procedures

- Grain size distribution – ASTM D422-63: Standard Test Method for Particle-Size Analysis of Soils (dispersion of soil sample using air-jet dispersion tube).
- Atterberg limits – ASTM D4318-05: Liquid Limit, Plastic Limit, and Plasticity Index of Soils (using the wet preparation method and Method A (multi-point method)).
- Specific gravity – ASTM D854-06: Standard Test Methods for Specific Gravity of Soil Solids by Water Pyconometer (Method A procedure for oven-dried specimens).
- Soil classification (USCS) – ASTM D 2487-00: Standard Practice for Classification of Soils for Engineering Purposes
- Soil classification (AASHTO) – AASHTO M145: Standard Specifications for Classification of Soils and Soil-Aggregate Mixtures for Highway Construction Purposes.

A.6.2 Soil Compaction Characteristics

Compaction methods employed in this research include: impact, static, vibratory, and gyratory. A brief overview of the test procedures is described below.

A.6.2.1 Impact Compaction

Laboratory impact compaction tests were performed in accordance with the following standard procedures. An automated, calibrated mechanical rammer was used to perform these tests.

- Standard Proctor test – ASTM D698–00: Standard Test Methods for Laboratory Compaction Characteristics of Soil Using Standard Effort
- Modified Proctor test – ASTM D 1557–02: Standard Test Methods for Laboratory Compaction Characteristics of Soil Using Modified Effort

A.6.2.2 Vibratory Compaction

Vibratory compaction tests were performed to determine the maximum and minimum index densities of granular soil samples in accordance with the following standard procedures. Tests were performed at different moisture contents.

- Maximum index density – ASTM D4253-00: Standard Test Method for Maximum Index Density and Unit Weight of Soils using a Vibratory Table.
- Minimum index density – ASTM D4254-00: Standard Test Method for Minimum Index Density and Unit Weight of Soils and Calculation of Relative Density.

A.6.2.3 Static Compaction

A standard test procedure is currently not available for performing static compaction tests. Two compaction molds that are custom made similar to Proctor tests (101.6 mm [4 in] diameter x 116.4 mm [4.583 in] height mold and a 152.4 mm [6 in] diameter x 116.4 mm [4.583] height molds) were used for these tests. Following the same criteria as ASTM D698 and D1557, the mold size was selected from the particle size distribution. Prior to compaction testing, samples were moisture conditioned and left to mellow as suggested in ASTM D698. Moist soil (approximately 2500 gm [5.5 lb] for 101.6 [4 in] mm mold and 5200 gm [11.5 lb] for 152.4 mm [6 in] mold) was placed in the mold in one lift and compacted using a manual hydraulic compression device. A load cell and two LVDT's connected to a computer with data acquisition system were setup such that soil deformation and the corresponding applied load were continuously recorded during the test.

A.6.2.4 Gyratory Compaction

A procedure for performing gyratory compaction tests on base and subgrade materials was suggested by McRae (1965). Recommendations on gyratory variables (applied pressure, angle, number of gyrations, gyration rate) are not yet standardized. Smith (2000), Ping *et al.* (2003), and Kim and Labuz (2006) used vertical applied stresses ranging from 200 kPa to 1380 kPa (29-200 psi), 1.0 to 1.25 degree gyration angle, 30 – 90 gyrations, and at a rate of 20 to 30 gyrations per minute for base and subgrade materials in their research. Vertical pressures of 600 kPa (87 psi), constant gyration angle of 1.25 degree, 50 gyrations, and at a rate 30 gyrations per minute were used in this study. The machine used in this study is a Pine Superpave Gyratory compactor.

A.6.3 Resilient Modulus and Shear Strength

Resilient modulus tests were performed in general accordance with AASHTO T-307 (1999), *"Standard Method of Test for Determining Resilient Modulus of Soils and Aggregate Materials"*. The Geocomp automated resilient modulus test setup was used in this study (*see* Marr *et al.* 2003 for details of this system). In the test setup, the LVDT is mounted to the piston rod to measure strain values in the sample during the test. According to Marr *et al. (*2003), the use of one versus two LVDT's (two LVDT's is suggested in AASHTO T-307) does not introduce error as the LVDT's rest on a rigid surface.

Resilient modulus is a highly stress-dependent parameter (Huang 1993). Many non-linear models have been proposed to incorporate the effects of stress levels and predict resilient modulus. Some of the popular models include the power-law model for granular soils (Monismith et al., 1971) and the deviator stress model for cohesive soils (Mohammad and Puppala, 1995). In reality, most soils exhibit the effects of increasing stiffness with increasing confinement and decreasing stiffness with increasing shear stress (Andrei *et al.* 2004). Witczak and Uzan (1988) proposed a "universal" model that combines both of these effects into a single equation (Equation A.1). Regression coefficients presented for the M_r tests performed in this study are based on this "universal" model. Tests were performed on compacted samples or Shelby tube samples, using standard conditioning and loading sequences suggested in the AASHTO T-307 for subgrade and base course materials. Summary results based on the average of the last five cycles of a loading sequence are output by the Geocomp Resilient Modulus software. Regression coefficients of the "universal" model are also shown in the summary chart provided by the software. Following the resilient modulus test, an unconsolidated undrained test (UU) was performed. The UU test was performed up to a maximum of 5% strain in the sample, or failure, whichever occurs first.

$$M_r = k_1 P_a \left(\frac{\theta}{P_a} \right)^{k_2} \left(\frac{\sigma_d}{P_a} \right)^{k_3} \quad \text{(A.1)}$$

where:
k_1, k_2, k_3 = regression coefficients, with $k_1 > 0$, $k_2 \geq 0$, and $k_3 \leq 0$.
θ = sum of principle stresses or bulk stress ($\sigma_1 + \sigma_2 + \sigma_3$)
P_a = atmospheric pressure, same units as M_r and θ
σ_d = deviator stress, same units as M_r and θ

A.6.3.1 Granular Soil Specimen Preparation

For impact compaction, the samples were compacted in six layers of equal mass and thickness (33.9 mm [1.335 in]). Each layer was compacted using the standard Proctor hammer until a target density was achieved (see Figure A.1a). Vibratory compaction was also performed in six layers of equal mass and thickness. Vibratory compaction was achieved using an electric rotary drill hammer (see Figure A.1b). The compaction process was continued until the predetermined density was reached. After compaction, a filter paper, a porous stone and the top platen were placed on the sample, and the rubber membrane was rolled off the split mold. Two O-rings were placed on the top platen to secure the membrane. Vacuum pressure was applied to the specimen and the split mold was removed. The triaxial chamber was then assembled for testing.

A.6.3.1 Non-Granular Soil Specimen Preparation

Static compaction was used in preparing cohesive soil specimens following the procedure suggested in AASHTO T-307 for Type 2 soils. Specimens were prepared to achieve a target density at a selected moisture content. Specimens were compacted in five 14.2 mm (0.559 in) thick layers statically using a hydraulic jack (see Figure A.2a) with the aid of spacer plugs. Each layer consisted of an equal mass of material. The mold was inverted after compacting each layer, and the layer was scarified before placing a new layer. For impact compaction, the specimens were also compacted in five layers of equal mass and thickness (14.2 mm [0.559 in]). Each layer was compacted using a Marshall Hammer with the aid of spacer plugs (see Figure A.2b). Similar to the static compaction method, the mold was inverted after compaction of each layer and the layer was scarified before placing a new layer. Impact blows were applied until the plug was level with the top of the sample mold. Vibratory compaction was also performed in five layers of equal mass and thickness (14.2 mm [0.559 in]). A new layer was placed directly on top of the previous layer without inverting the mold. Vibratory compaction was achieved using an electric rotary drill hammer. The compaction process was continued until reaching a predetermined target height. This process is shown in Figure A.2c. After compaction, the specimens were extruded into the extrusion mold and weighed for dry unit weight calculations. The specimens were then placed in the triaxial chamber with membranes and O-rings for testing.

(a) (b)

Figure A.1: Different compaction procedures for cohesionless soil specimen preparation: (a) impact, and (b) vibratory

(a) (b) (c)

Figure A.2: Different compaction procedures for cohesive soil specimen preparation: (a) static, (b) impact (Marshall Hammer), and (c) vibratory

A.7 SPOT TEST MEASUREMENT METHODS

A variety of in-situ point measurement devices were used in this research. A brief description of each test device and the associated test method are provided below.

A.7.1 Moisture – Dry unit weight

A calibrated nuclear moisture-density gauge (NG) device was used to provide rapid measurements of soil dry unit weight and moisture content. Tests were performed following ASTM WK218 *"New Test Method for In-Place Density and Water (Moisture) Content of Soil"*. Generally, two measurements of moisture and dry unit weight were obtained at a particular location and an average value is reported. Probe penetration depths varying from 200 mm (8 in.) to 300 mm (12 in.) were used in performing the tests. In addition to *NG* tests, 72.6 mm diameter (2.86 in.) drive cylinders (*DC*) were also obtained to measure the in-situ moisture and dry densities. *DC* tests were performed in accordance with ASTM D 2937 *"Standard Test Method for Density of Soil in Place by the Drive-Cylinder Method"*.

A.7.2 Dynamic Cone Penetrometer

Dynamic cone penetrometer (DCP) is used to measure of strength characteristics of compacted fill materials according to ASTMD 6951 *"Standard Test Method for Use of Dynamic Cone Penetrometer for Shallow Pavement Applications"*. The test involves dropping an 8 kg (17.64 lb) hammer 575 mm (22.64 in) and measuring the penetration rate of a 20 mm (0.787 in) diameter cone. Dynamic penetration index (DPI) with units of mm/blow is estimated from the test. The DPI values are inversely related to penetration resistance (i.e. soil strength). DCP testing is well discussed in literature (e.g. Gabr *et al*. 2000; Livneh *et al*. 2000) with a general focus of correlating DCP index to other measures of pavement performance (e.g. CBR, modulus). An average DPI value of the compaction layer was calculated as the ratio of thickness of the compaction layer and cumulative number of blows required to reach that penetration depth. CBR was then determined using following equation presented in ASTM D6951.

$$\text{CBR} = \frac{292}{(\text{DCPI})^{1.12}} \tag{A.2}$$

A.7.3 Light Weight Deflectometer (LWD)

Three different light weight deflectometers (LWDs) were used in this study to determine elastic modulus: (a) Zorn, (b) Keros, and (c) Dynatest. A 10 kg (22.05 lb) drop weight is used to produce a dynamic load on the bearing plate. The Keros and Dynatest models use a load sensor to measure the load pulse, and a geophone at the center of the plate to measure the corresponding soil deflection. The Zorn model assumes a contact plate stress based on calibration of the falling weight, and plate deflection is obtained from an in-built accelerometer in the loading plate. Using the applied contact stress and deflection values, the elastic modulus is then calculated as:

$$E_{LWD} = \frac{(1-v^2)\sigma_0 r}{d_0} \times f \tag{A.3}$$

Where, E_{LWD} = elastic modulus determined using *LWD* (MPa), d_0 = measured settlement (mm), v = Poisson's Ratio (0.4), σ_0 = applied stress (MPa), r = radius of the plate (mm), f = shape factor assumed as $\pi/2$. The resulting E_{LWD} values differ significantly with size of loading plate and type of LWD device (see Vennapusa and White. 2009). To differentiate the E_{LWD} values between different devices and setups the following terminology is used in presentation of the results:

- $E_{LWD\text{-}D2or3} - E_{LWD}$ by a Dynatest device setup with 200-mm or 300-mm plate diameter.
- $E_{LWD\text{-}K2or3} - E_{LWD}$ by a Keros device setup with 200-mm or 300-mm plate diameter.
- $E_{LWD\text{-}Z2or3} - E_{LWD}$ by a Zorn device setup with 200-mm or 300-mm plate diameter.

A.7.4 Static Plate Load Test (PLT)

Stress-controlled static plate load tests were performed for elastic modulus (E_{VI}) of compacted materials using a 300-mm (12 in) plate, a 90-kN (10.116 ton) load cell, and three 50 mm (1.969 in) linear voltage displacement transducers (setup shown in Figure A.3a). E_{VI} was calculated from the interpretation of load-deflection curves shown in Figure A.3b.

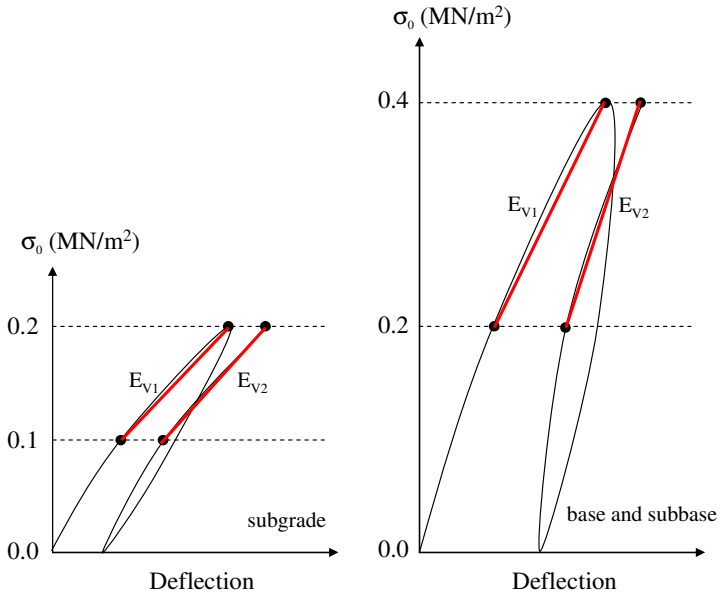

Figure A.3: Static plate load test data modulus scheme for subgrade, subbase, and base materials

A.7.5 Soil Stiffness Gauge (SSG)

The soil stiffness gauge is a nondestructive test device for obtaining the in-situ deformation characteristics of soil. The device, which is also referred to as the GeoGauge, rests on the soil surface and vibrates at 25 frequencies ranging from 100 to 196 Hz. The vibrating device produces small dynamic forces and soil deflections, from which soil modulus can be calculated as (Humboldt Mfg. Co. 2000):

$$E_{SSG} = \frac{F(1-\nu^2)}{\delta(1.77\,r)} \qquad \text{(A.4)}$$

where F is a dynamic force caused by the vibrating device, δ is the deflection measured with a geophone, ν is Poisson's ratio, and r is the radius of the annular ring. Only modulus from the soil stiffness gauge (E_{SSG}) was used for developing correlations with other soil properties, because stiffness and modulus from the SSG are related through a linear relationship, dependent on Poisson's ratio (ν = 0.40) and the diameter of the annular ring of the device (Humboldt Mfg. Co. 2000).

A.7.6 Clegg Impact Hammer

Clegg impact tests were performed on select test beds for obtaining the measure of soil stability. The Clegg impact value ($CIV_{4.5\text{-}kg}$ or $CIV_{20\text{-}kg}$) is derived from the peak deceleration of a 4.5 kg (9.92 lb) or 20 kg (44.09 lb) hammer free falling 450 mm (17.717 in) in a guide sleeve for four consecutive drops.

A.7.6 Surface Wave Testing

Surface wave testing (Nazarian et al., 1999, Ryden and Lowe, 2004) was performed on chosen test beds. The velocity of surface waves is measured using multiple hammer impacts at different distances from a fixed accelerometer on the surface (see Figure A.4). The surface wave technique can be used to profile the shear wave velocity (or modulus) versus depth to several meters below the surface using a

backcalculation procedure (inversion) (Ryden and Park, 2006). Alternatively, a mean value analysis of a uniform top layer (e.g., a lift of soil) can be performed directly from the raw data (Nazarian et al. 1999).

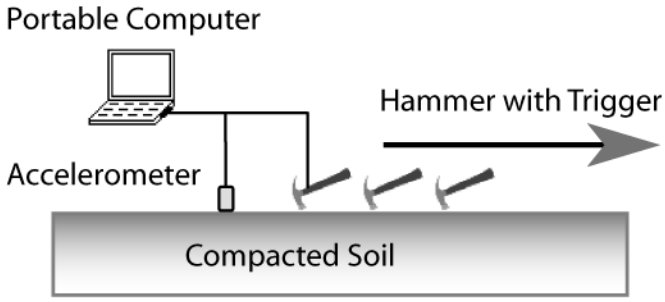

Figure A.4. Schematic illustration of surface wave measurements using one source and one receiver

A.8 LABORATORY TEST RESULTS AND DISCUSSION

A.8.1 Compaction Test Results

A cohesive material (mixed subgrade B) and a granular base material (class 5 base) from MnROAD project site were selected to study compaction characteristics of these soils using different compaction methods. This study was intended to identify the differences in moisture-density relationships with different compaction methods. Figures A.5 and A.6 present moisture-density curves using static, impact, vibratory, and gyratory compaction methods for the mixed subgrade B and class 5 base materials, respectively.

A.8.1.1 Subgrade Materials

Figure A.5a show for subgrade clay material that increasing the impact compaction energy increases the maximum dry unit weight and lowers the optimum moisture content. The portion of the moisture-dry unit weight curves on the wet side of optimum generally parallel the zero air void line (100% saturation). The points of optimum moisture content also tend to parallel the zero air void line. These relationships are commonly seen for fine-grained soils subject to impact compaction test methods.

The moisture-density curves from static compaction tests are shown in Figure A.5b. Similar to impact test results, the static test results show that with increasing applied stresses (compaction energy) the maximum dry unit weight increases and the optimum moisture content decreases. Further, with increasing moisture content, the applied stress to achieve a dry unit weight tends to decrease. Similar behavior has been observed by others (e.g. Lambe and Whitman 1969, Bell 1977, and Zhang *et al.* 2005). The maximum dry unit weight achieved with an applied stress of 4000 kPa (580 psi) is approximately 106% of maximum dry unit weight and +0.8% of optimum moisture content from the standard Proctor test.

Figure A.5c shows the moisture-density curve for the vibratory compaction test. Vibration was applied for a standard duration time of 8 minutes. An unusual moisture-density curve was observed from this test. The densities generally decrease up to about 15% moisture content (which is close to standard Proctor optimum moisture content) and then increase thereafter up to about 23% moisture content and then again decreased with increasing moisture content. Above 23% moisture content, the curve parallels the zero air void line. Low densities at moisture contents dry of optimum are typically observed in cohesionless sands due to "bulking". This phenomenon is typically not expected for fine-grained cohesive soils. A maximum dry unit weight of about 95% of the standard Proctor maximum dry unit weight was

achieved for the air dry sample at 2.7% moisture. Webster (1984) performed similar tests using a vibratory compactor on fine-grained cohesive soils (classified as CL), and showed a similar moisture-density curve with maximum densities at air dry moisture contents.

Results from the gyratory compaction test are shown in Figure A.5d. A constant vertical pressure (σ_v) of 600 kPa (87 psi) with gyration angle 1.25 degrees, and 50 gyrations at the rate of 30 gyrations per minute were applied during the test. The optimum moisture content from the test (14.7%) is close to the standard Proctor optimum (15.0%); however, the maximum dry unit weight is approximately 108% of the standard Proctor maximum dry unit weight. Similar to the static test, the optimum moisture is closer to the zero air void line. The curve on the wet side of optimum tends to parallel the zero air void line.

A.8.1.2 Class 5 Base Material

Figure A.6a shows the moisture-density relationships for impact compaction tests at standard and modified Proctor energies. As shown, no significant variations in density with increasing moisture content and compaction energy are realized. Maximum dry unit weight determined by modified Proctor method is only about 103% of the standard Proctor maximum dry unit weight. The curves on the wet side of optimum generally tend to parallel the zero air void line.

The moisture-density curves from static compaction tests at applied stresses varying from 500 kPa to 2500 kPa (73-363 psi) are shown in Figure A.6b. With increase in moisture, the applied stress to achieve a dry unit weight tends to decrease. Approximately 96% of the standard Proctor maximum dry unit weight is achieved at 9.6% moisture with 2,500 kPa (363 psi) applied stress. Porter (1930) indicated that with a static pressure of about 13,800 kPa (2002 psi), the moisture density results were similar to impact compaction tests on some granular materials. Maximum stress applied in these tests was about 2,500 kPa (363 psi). Greater applied stress could result in higher dry unit weights, however, an applied stress of 2,500 kPa (363 psi) is itself considered higher than what is typically observed during construction. Therefore, no attempt was made to apply additional vertical stresses.

Figure A.6c shows the moisture-density curve for a vibratory compaction test. The bulking phenomenon can be observed at about 3% moisture content from the figure. The maximum dry unit weight is approximately 102% of the standard Proctor maximum dry unit weight. Optimum moisture content is approximately -1% of the standard Proctor optimum. The curve on the wet side of optimum tends to parallel the zero air void line.

Results from the gyratory compaction test are shown in Figure A.6d. The optimum moisture content is less well defined, but similar to the standard Proctor optimum. The maximum dry unit weight is approximately 104% of the standard Proctor maximum dry unit weight. The moisture-dry unit weight curve approached the zero air void line.

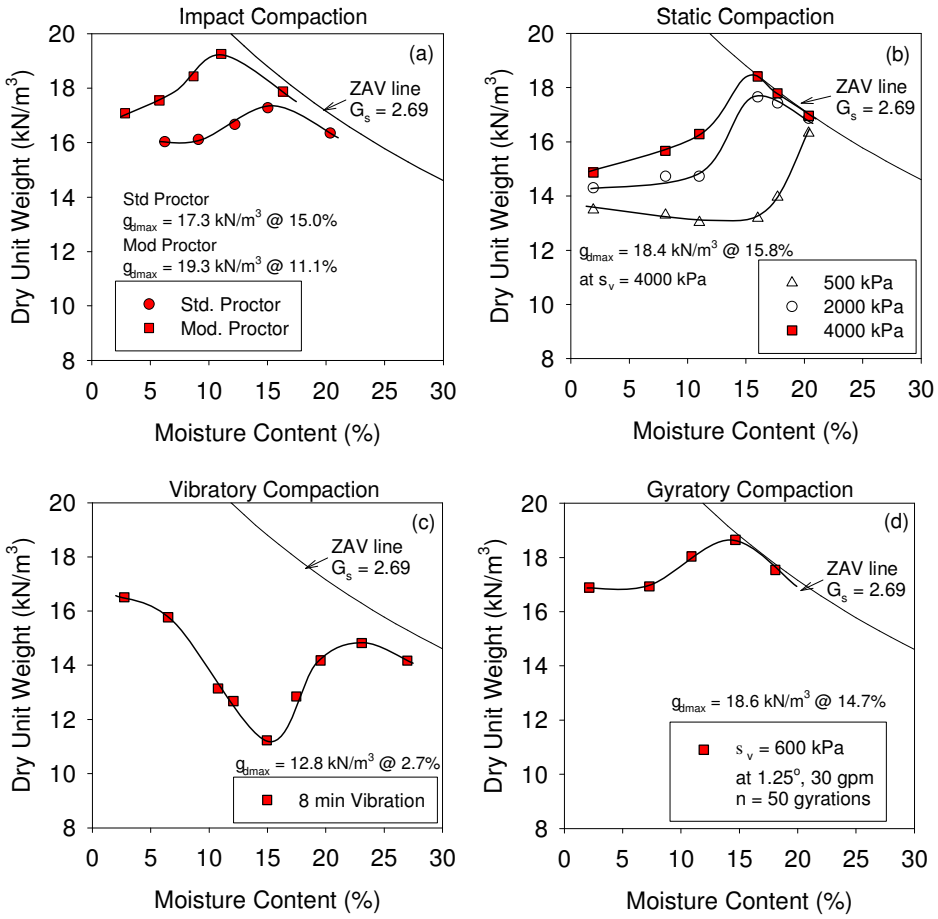

Figure A.5: Moisture density relationships for mixed subgrade B material using (a) impact, (b) static, (c) vibratory, and (d) gyratory compaction methods

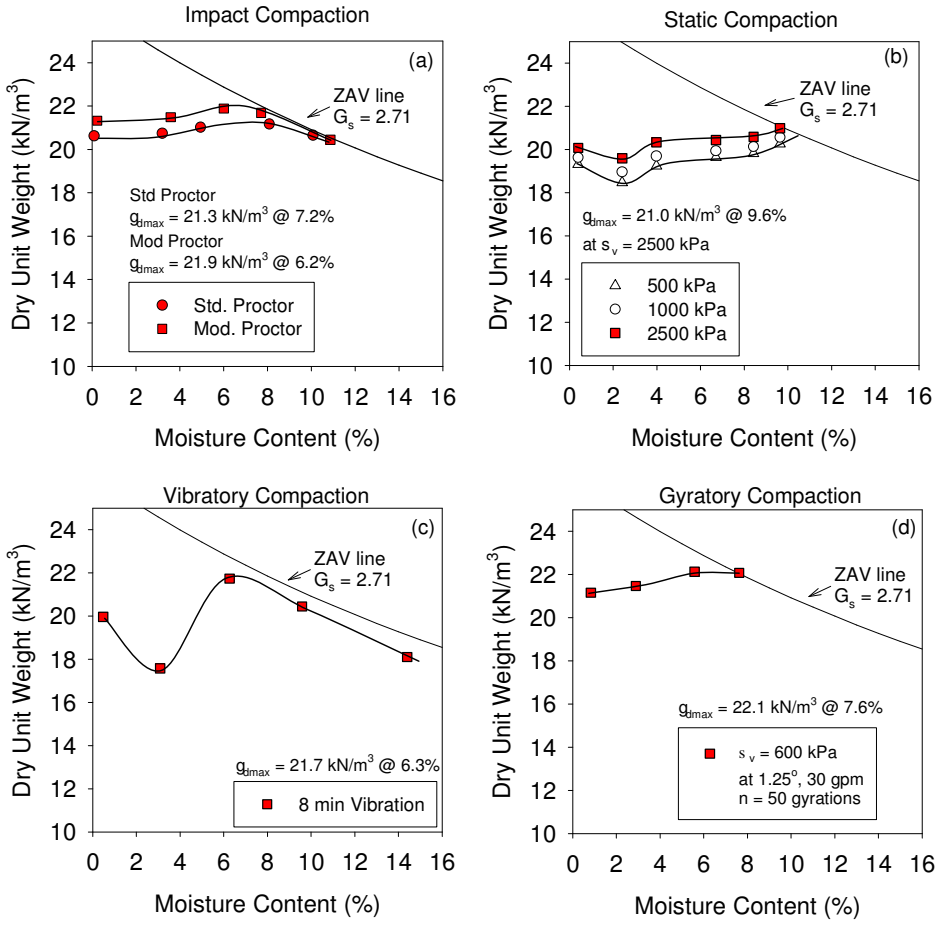

Figure A.6: Moisture density relationships for class 5 base material using (a) impact, (b) static, (c) vibratory, and (d) gyratory compaction methods

A.8.2 Relationship between Moisture-Density and Resilient Modulus

Moisture and density affect the resilient properties of soil. Results reported by Seed *et al.* (1962), Tanimoto and Nishi (1970), Thomson and Robnett (1979), and Lee *et al.* (1997) showed that M_r is higher on the dry side of optimum moisture content and decreases with increasing moisture content. Lee *et al.* 1997 showed that keeping moisture constant, increasing density can increase M_r. The relationships between moisture, density and resilient modulus vary, however, widely between different soils.

To establish target M_r values relating to moisture and density, laboratory M_r tests were performed on materials prepared at a wide range of moisture contents and dry unit weights. Tests were performed on three cohesive subgrade materials, two granular subgrade materials, and five granular base materials. The standard Proctor and modified Proctor moisture and density values were generally used as target values during sample preparation. The M_r tests were performed following the testing sequences described in AASTHO T-307 procedure – Type 2 for cohesive and granular subgrade materials and Type 1 for granular base materials. The cohesive subgrade materials were compacted using static compaction method and granular subgrade and base materials were compacted using vibratory compaction method as suggested in AASHTO T-307.

A.8.2.1 Effects of Stress State on Resilient Modulus

Results showing effects of deviator and confining stresses are presented in Figure A.7 for a cohesive subgrade material, and in Figure A.8 for a granular base material. Summary test results for Phase I and Phase II soils are presented in Tables A.11 and A.12 along with the constuitive model coefficients (Equation A.1) 4.1.

Figure A.6 shows results of a cohesive subgrade material compacted to standard Proctor densities at moisture conditions varying from -7.5% of optimum (top left corner) to +6% of optimum (bottom right corner). The results show two commonly observed effects on fine-grained cohesive soils: (a) increasing moisture content decreases the M_r for any given stress condition; and (b) increasing deviator stress generally decreases M_r. Some differences with respect to these typical behaviors were observed in the results. For samples prepared at dry state of optimum (-7.5%), the confining stress effects the Mr values more than the deviator stress. Increasing confining stress tends to increase the M_r value (up to about 1.5 times), while increasing deviator stress did not produce a significant change in M_r. On the other hand, as the moisture increases, for example at +2% of optimum, the confining stress only slight effected M_r while increasing deviator stress caused a significant decrease in M_r (up to about 2 times). According to Witczak and Uzan (1988), the model coefficients k_1 and k_2 are > 0 and k_3 is ≤ 0. The smaller the k_3 value the greater the influence of deviator stress. Some samples exhibited a positive k_3 value which suggests an increase in M_r with increasing deviator stress. This behavior is sometimes observed in some stiff granular materials, but is not typical for fine-grained cohesive soils.

For granular base material shown in Figure A.7 shows that the effect of confining stresses on M_r is significantly more than for deviator stress. An increase in confining stress caused an increase in M_r for all three samples (by 2 to 4 times). Also, an increase in deviator stress generally up to about 41 kPa showed an increasing trend in M_r and then decrease or no change in M_r with further increase in deviator stresses up to about 69 kPa (10 pisi). A similar trend of M_r with deviator stress was reported by Brown (1974) and Zeghal (2004). However, this trend is not always true for all granular materials. For example, Hicks (1970) found that for granular materials the confining stress has a most significant effect while deviator stress has almost no effect on M_r. Morgan (1966) found that increasing deviator stresses caused a decrease in M_r for granular materials.

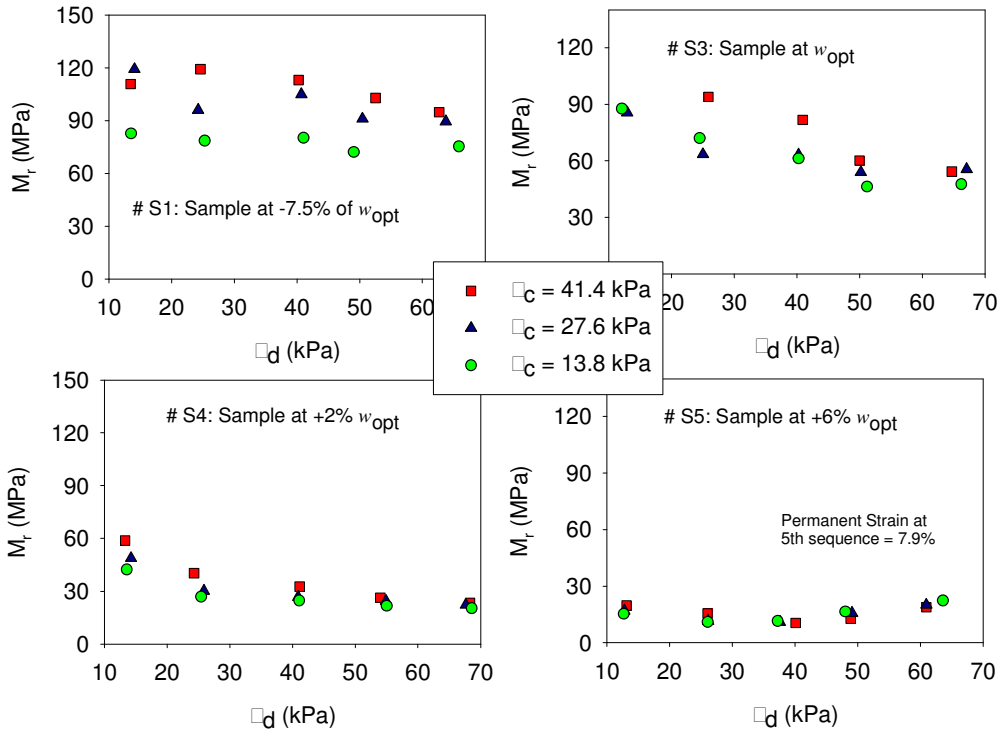

Figure A.7 Effect of σ_c and σ_d on compacted MN10 subgrade material at different target w-γ_d

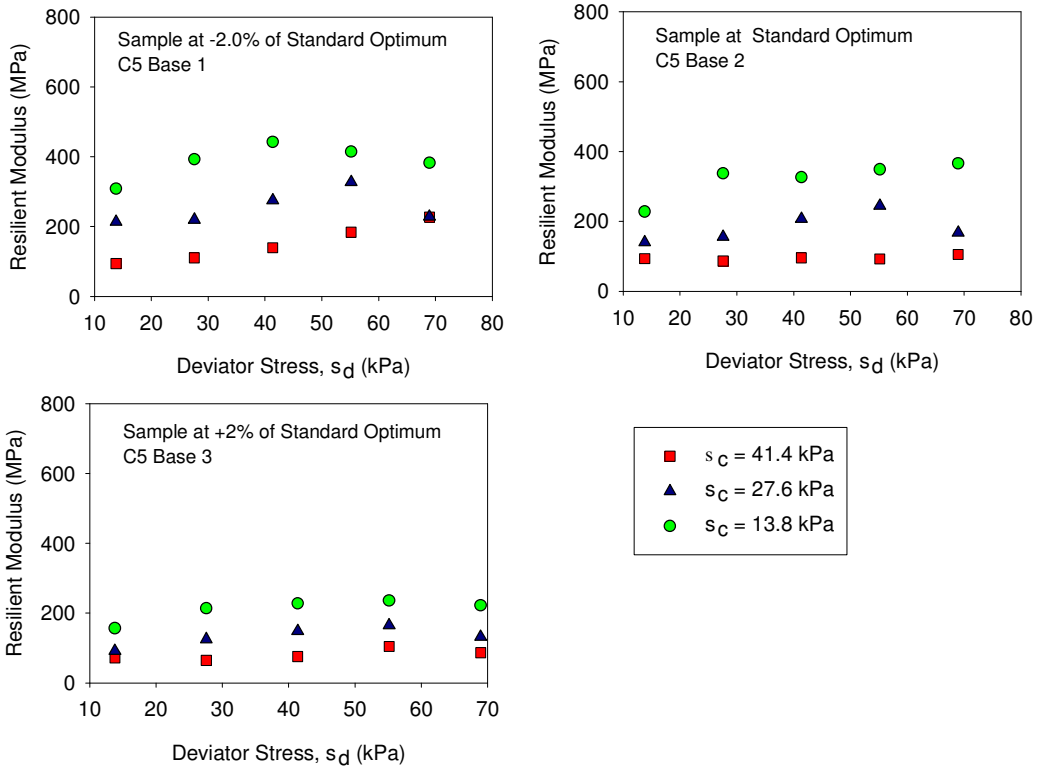

Figure A.8: Effect of confining and deviator stresses on class 5 base material

Table A.11: Summary of resilient modulus test results and model coefficients: Phase I MnROAD project soils

Material [classification]	Series	w%	γ_d (kN/m^3)	S%	M_r at σ_d = 68.9 kPa and σ_c = 41.4 kPa	k_1	k_2	k_3	R^2
Borrow Subgrade MN10/11 (CL) (A-6(5))	S	8.9	16.10	37.5	86.5	675.4	0.45	-0.24	0.8
	S	11.9	16.80	56.1	87.7	706.7	0.00	-0.14	0.4
	S	16.2	17.40	84.4	69.9	431.5	0.17	-0.34	0.7
	S	18.5	16.80	87.2	16.0	149.6	0.35	-0.60	1.0
	S	22.0	15.70	86.9	–[a]	–[a]	–[a]	–[a]	–[a]
	M	8.8	16.90	42.2	126.2	969.6	0.13	-0.11	0.3
	M	11.1	19.30	81.3	217.0	1755.9	0.17	0.08	0.5
	M	13.6	18.30	82.8	141.6	952.6	-0.01	-0.04	0.5
	M	18.0	16.70	83.5	16.6	159.8	0.43	-0.50	1.0
	M	20.8	15.70	82.2	–[a]	–[a]	–[a]	–[a]	–[a]
Mixed Subgrade (CL) (A-6(5))	S	6.1	16.30	26.5	135.9	1059.3	0.11	0.09	0.2
	S	8.4	16.70	38.9	114.9	1363.6	-0.14	0.02	0.2
	S	11.5	17.50	60.9	107.5	707.1	0.17	-0.30	0.7
	S	14.6	17.90	82.8	67.9	560.4	0.00	-0.29	0.4
	S	23.3	15.30	86.5	–[a]	–[a]	–[a]	–[a]	–[a]
	M	11.6	19.50	88.3	267.0	2758.5	-0.05	0.12	0.2
	M	13.5	18.70	88.3	158.1	1234.1	0.23	0.08	0.4
	M	20.8	15.80	83.5	–[a]	–[a]	–[a]	–[a]	–[a]

[a] Samples with strains generally > 5% - test terminated at an intermediate sequence

Table A.12: Summary of resilient modulus test results and model coefficients – Phase II soils

Material [classification]	Series	w%	γ_d (kN/m^3)	S%	M_r at σ_d = 68.9 kPa σ_c = 41.4 kPa	k_1	k_2	k_3	R^2	τ_{max} (kPa)
Colorado Subgrade CO3 (CL) (A-6(7)[a]	–	10.4	18.79	71.9	32.813	255.62	0.351	-0.027	0.7	–
	–	10.3	18.19	63.6	50.017	394.03	0.166	-0.307	1.0	110.5
	–	14.0	18.41	90.0	35.605	257.98	0.391	-0.148	0.7	96.9
	–	14.0	17.96	82.9	22.742	123.79	0.614	-0.517	1.0	112.9
	–	16.7	17.09	84.9	9.148	64.37	0.291	-0.391	0.9	62.7
	–	17.1	17.14	87.7	8.516	71.56	0.122	-0.213	0.8	86.8
Colorado Base CO17 to CO20 (SP-SM) (A-1-a)	M	1.1	20.25	10.3	142.375	459.61	0.631	-0.092	1.0	121.3
	M	3.2	20.63	32.6	168.272	692.36	0.423	0.064	0.9	239.7
	M	5.1	21.25	60.5	205.587	454.86	0.838	-0.111	1.0	268.8
	M	7.6	21.38	93.3	151.145	607.70	0.517	-0.093	0.9	215.3
	M	8.5	20.88	91.9	92.501	284.74	0.601	0.013	1.0	226.1
	S	0.9	19.37	7.0	141.194	382.93	0.796	-0.234	1.0	137.0
	S	3.8	19.54	30.5	151.911	548.37	0.556	-0.060	0.9	138.1
	S	6.5	20.70	67.3	154.611	429.18	0.704	-0.081	0.9	226.1
	S	5.6	18.52	36.8	124.434	340.43	0.769	-0.191	1.0	226.1
	S	7.9	19.73	65.9	121.615	501.95	0.436	0.036	0.9	127.8
Maryland Subgrade MD2 to MD5 (SM) (A-2-4)	M	5.8	18.85	40.5	86.8	628.118	0.428	-0.090	0.8	967.4
	M	7.8	19.46	61.5	67.6	516.288	0.323	-0.125	0.8	653.1
	M	9.5	20.06	85.1	40.2	138.734	1.112	-0.869	0.9	309.6
	M	11.7	19.32	89.7	36.0	164.821	0.872	-0.534	0.9	310.5
	M	13.7	18.44	88.6	33.1	175.637	0.771	-0.321	1.0	168.7
	S	5.8	17.04	29.2	88.5	505.690	0.866	0.030	0.8	492.7
	S	7.8	17.55	42.9	64.7	325.376	0.684	-0.606	0.9	272.5
	S	9.4	16.49	43.2	40.1	240.081	0.594	-0.305	0.7	187.8
	S	11.6	18.91	82.0	37.5	200.529	0.712	-0.397	0.8	258.0
Maryland Base MD6 to MD14 (SP-SM) (A-1-a)	M	1.2	21.46	15.0	234.0	725.910	0.655	-0.098	1.0	155.9
	M	2.2	21.52	28.0	233.3	833.244	0.526	0.008	0.9	313.4
	M	3.6	22.12	54.4	143.0	669.687	0.323	0.126	0.9	342.8
	M	4.5	21.98	65.3	166.2	514.289	0.601	0.008	0.9	243.7
	M	4.4	22.92	86.9	170.3	484.095	0.644	0.010	1.0	145.7
	M	5.2	22.12	78.6	115.5	389.972	0.537	0.043	1.0	164.4
	S	1.1	20.66	11.3	167.9	560.435	0.587	-0.041	0.9	95.9
	S	2.3	20.47	22.6	176.6	701.714	0.475	-0.001	0.9	124.8
	S	3.8	22.09	56.9	201.8	618.231	0.621	-0.020	0.9	213.2
	S	4.9	21.98	71.1	124.1	469.561	0.497	0.006	0.9	76.8
Florida Subgrade FL23 (SP-SM) (A-3)	M	0.3	15.50	1.2	84.5	589.383	0.518	-0.035	0.8	77.7
	M	3.5	15.82	14.4	93.7	642.263	0.576	0.016	0.8	71.0
	M	5.8	16.07	24.9	102.3	795.917	0.474	0.175	0.9	66.5
	M	8.2	16.26	36.3	95.4	713.973	0.493	0.105	0.6	71.7

Florida Subgrade FL23 (SP-SM) (A-3)	M	13.2	15.68	53.2	83.5	547.011	0.631	-0.009	0.7	42.8
	S	0.1	15.05	0.4	65.8	310.281	1.024	-0.205	0.9	42.8
	S	3.9	15.36	14.9	79.8	461.408	0.748	-0.137	0.8	93.9
	S	5.8	15.77	23.7	106.6	896.371	0.431	0.304	0.8	69.8
	S	8.3	15.91	34.7	87.7	599.021	0.611	0.066	0.8	97.6
	S	15.9	14.86	56.2	83.7	595.728	0.532	0.041	0.7	55.0
	–[b]	3.4	16.76	16.3	71.2	505.673	0.512	0.002	0.9	105.3
	–[b]	9.2	15.38	35.3	61.8	483.276	0.347	-0.023	0.7	81.2
	–[b]	13.0	16.65	61.4	95.0	514.910	0.830	-0.166	0.8	105.1
Florida Base FL19 (SM) (A-1-b)	–[b]	4.9	17.42	26.4	190.2	899.068	0.407	-0.044	0.8	251.3
	–[b]	7.8	18.54	51.4	202.4	668.296	0.649	-0.149	0.9	474.5
	–[b]	9.5	17.99	56.6	236.1	447.850	1.020	-0.306	0.8	267.5
	–[b]	2.4	16.59	11.2	181.3	767.271	0.435	0.013	0.9	121.2
	–[b]	7.7	16.86	37.7	206.4	948.452	0.426	-0.052	0.8	237.2
	–[b]	12.0	18.07	72.5	167.9	575.074	0.667	-0.220	1.0	285.2
North Carolina Subgrade NC2 (A-4) SM	M	5.8	17.94	34.2	28.6	171.988	0.585	-0.306	0.8	150.5
	M	8.4	18.90	59.3	41.7	268.421	0.536	-0.213	0.6	400.4
	M	11.1	18.87	77.9	35.5	287.034	0.139	-0.286	0.7	287.5
	M	12.5	18.74	85.5	20.3	166.314	0.255	-0.062	0.9	309.6
	M	14.6	18.13	89.2	28.1	166.914	0.548	-0.397	0.9	187.1
	M	16.7	17.42	89.9	23.0	124.512	0.676	-0.431	0.6	152.5
	S	8.4	18.90	59.3	28.3	112.541	1.003	-0.680	0.9	192.2
	S	11.0	17.30	58.0	31.9	201.400	0.517	-0.294	0.8	183.2
	S	12.8	17.37	68.3	28.0	173.319	0.464	-0.438	0.8	187.5
	S	14.7	17.04	74.1	25.7	132.608	0.669	-0.568	0.9	177.8
	S	16.7	16.65	78.8	19.8	94.392	0.809	-0.534	0.9	109.9
	–[b]	4.9	18.74	33.5	44.1	273.713	0.572	-0.248	0.9	467.6
	–[b]	4.6	16.51	21.2	34.7	256.098	0.323	-0.213	0.5	165.9
	–[b]	10.6	18.07	64.0	31.4	246.222	0.235	-0.206	0.7	293.9
	–[b]	11.0	16.65	51.9	27.9	148.703	0.763	-0.324	0.9	97.9
	–[b]	17.9	16.64	84.4	21.2	124.644	0.643	-0.266	0.7	99.5
North Carolina Base NC4 (A-1-a) SP-SM	–[b]	0.3	20.83	3.2	145.7	357.413	0.782	-0.107	1.0	194.1
	–[b]	2.5	20.83	26.7	171.4	480.206	0.641	0.030	1.0	218.3
	–[b]	3.9	21.24	46.2	175.8	497.435	0.683	-0.060	1.0	224.2
	–[b]	6.0	21.82	83.1	159.4	457.635	0.647	-0.005	1.0	258.2
	–[b]	7.0	21.74	94.7	129.1	280.292	0.831	-0.079	1.0	271.9
	–[b]	0.2	20.28	1.9	118.7	329.168	0.669	-0.013	1.0	138.5
	–[b]	2.5	20.47	24.5	139.2	405.771	0.606	0.058	1.0	188.6
	–[b]	3.9	20.85	41.9	155.9	518.770	0.525	0.081	1.0	192.9
	–[b]	6.0	21.27	71.6	128.0	511.460	0.505	-0.064	0.9	224.7
	–[b]	9.0	20.63	91.7	106.4	290.013	0.705	-0.065	0.9	111.5
	–[b]	1.2	21.65	15.8	223.4	607.960	0.724	-0.100	0.8	242.7
	–[b]	3.7	19.65	30.4	129.6	454.132	0.555	-0.028	0.9	124.4
	–[b]	3.2	21.63	42.0	181.2	516.713	0.741	-0.179	0.9	329.1
	–[b]	6.0	20.58	60.4	119.0	419.158	0.552	-0.028	1.0	157.5

[a] Shelby tube samples; [b] randomly selected points

A.8.2.2 Predicting Resilient Modulus from Moisture and Density

The AASHTO T-307 procedure involves a conditioning sequence followed by fifteen loading sequences with different applied deviator (σ_d) and confining stress (σ_c) combinations. Relationships to predict M_r as a function of moisture and density are presented below. These predicted M_r values could potentially be related to roller MV's. The stresses applied during roller compaction can be significantly higher than the applied stress levels in a M_r test, however. Therefore, M_r results at a representative stress condition of σ_d = 68.9 kPa (10.0 psi) and σ_c = 41.4 kPa (6.0 psi) only are presented below.

Figure A.9 shows the effect of moisture content and density on M_r of a cohesive subgrade material. M_r value corresponding to a triaxial sample compacted to a target moisture and dry unit weight are presented in this figure. The triaxial (M_r) samples are divided into two groups, S and M, where group S represent the samples compacted to target standard Proctor moisture-density values and group M represent samples compacted to target modified Proctor moisture-density values. According to AASHTO T-307 when a sample reaches a permanent strain of >5%, the test shall be terminated. For both materials, the samples with moisture contents greater than about 20% resulted in permanent strains >5%, generally before reaching the selected stress condition (σ_d = 68.9 kPa [10.0 psi] and σ_c = 41.4 kPa [6.0 psi]). These samples are highlighted in Figure A.9.

Based on the M_r values shown in Figure A.9, a multiple linear regression model as a function of dry unit weight and moisture content was developed (*see* Table A.13). The model resulted in R^2 values of 0.96 which indicates a strong correlation. Note that the M_r values for the samples with >5% permanent strain were not considered in the multiple linear regression analysis. Using the multiple regression relationship, contours of the predicted M_r are plotted as shown in Figures A.9. Since the parameters in the models are linear terms, the M_r contours are linear and parallel lines showing a reduction in M_r with increasing moisture content. It can be seen in Figure A.9 that the M_r values decrease rapidly along the moisture-dry unit weights curves on the wet side of optimum. These results indicate that a slight increase in moisture content over standard Proctor optimum (less than +3%) will decrease the M_r to about "zero". Additional samples with changes in moisture and dry unit weights on the wet side of optimum are warranted to help better define the contours in this region.

Results plotted in this manner can aid in determining target M_r values relating to moisture and dry unit weight, and also vise versa. Similar analysis was performed on the results obtained from tests on the other samples. A summary of multiple regression relationships are provided in Table A.13.

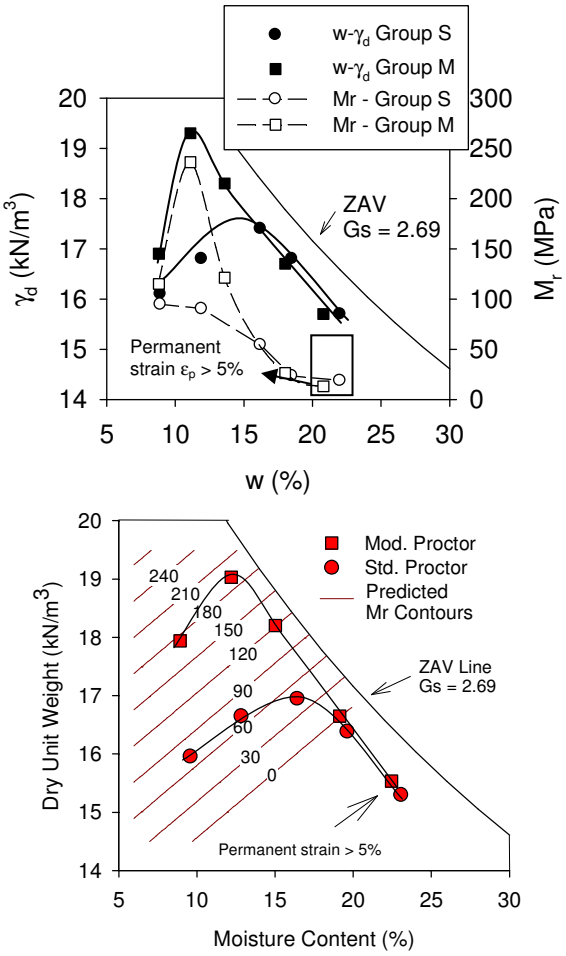

Figure A.9 Relationship between w-γ_d and M_r at σ_d = 68.9 kPa and σ_c = 41.4 kPa

Table A.13: Summary of moisture-dry unit weight- M_r relationships

Material	TB	USCS (AASHTO)	n	b_0	b_1	b_2	R^2
Model: $M_r^* = b_0 + b_1 w + b_2 \gamma_d$							
Non-granular subgrade	MN10,11	CL (A-6(5))	8	-593.33	-10.86	48.23	0.96
	CO3**	CL (A-6(7))	6	*limited number of samples*			
Granular subgrade	MD2, 3, 4,5	SM (A-2-4)	9	124.10	-7.56	0.03	0.85
	FL 23	SP-SM (A-3)	13		NS		–
	NC2	SM (A-2-4)	16	-28.48	-1.17	4.12	0.94
Granular base	CO17,18	SP-SM (A-1-a)	9	-248.29	-5.14	20.95	0.67
	MD6, 7, 8, 9, 11, 12, 13, 14	SP-SM (A-1-a)	10	-426.37	-30.09	32.19	0.62
	FL19	SM (A-1-b)	5	*limited number of samples*			
	NC4	SP-SM (A-1-a)	14	-512.01	-7.05	32.85	0.62

* for σ_d = 68.9 kPa and σ_c = 41.4 kPa; **ST samples

A.8.3 Influence of Compaction Method on Strength and Resilient Modulus

Resilient modulus (M_r) is commonly used as a measure of stiffness for unbound materials in the pavement structure. Following AASHTO T-307 standard Mr test procedure, specimens of fine-grained cohesive subgrade materials are statically compacted in five layers, while the new NCHRP 1-28 procedure implements impact compaction for fine-grained cohesive soils. As an alternate, kneading compaction is suggested in both standards. Vibratory or kneading compaction is suggested for granular materials. However, limited information was identified in the literature discussing the influence of compaction type on resilient properties of unbound materials. Elliott and Thornton (1988) found that cohesive soil samples compacted using static compaction have higher resilient modulus than those compacted using kneading compaction. Results from tests performed on granular materials by Zaman *et al.* (1994) using impact and vibratory compaction methods showed that the compaction type did not significantly influence the resilient modulus. Hoff *et al.* (2004) also indicated that no significant difference was observed between impact, vibratory, and gyratory compaction on M_r of a granular material.

As a preliminary investigation, the influence of compaction method on the strength and stiffness properties was studied on one cohesive subgrade material and one granular base material from the MnROAD project. M_r and UU shear strength tests were performed on mixed subgrade B and class 5 base materials following the AASHTO T-307 standard procedure. Specimens were compacted to target moisture contents and dry unit weights using different compaction methods. Static, impact, and vibratory compaction methods were used for the mixed subgrade B material, and impact and vibratory method for the class 5 base material.

A.8.3.1 Mixed Subgrade B Material

Samples were compacted to achieve a target of 100% standard Proctor maximum density (17.3 kN/m^3 [110.1 pcf]) at moistures -3%, 0%, and +3% of optimum moisture content (15.3%). Table A.14 provides summary M_r and UU test results and the constuitive model coefficients (Equation A.1). The mean M_r values and the coefficient of variation (COV) of the value within a test are also shown in Table A.14.

The mean M_r of statically compacted samples is lower than that for samples compacted using impact or vibratory methods (Figure A.10). This difference is substantial on the dry side of the optimum moisture content (-3%) with the static method resulting in M_r values two times lower compared to impact or vibratory methods. On the wet side of optimum, the impact and static methods have similar M_r values, while the vibratory method produced M_r values about 1.3 times higher than the other two methods. In general, no significant difference in the mean M_r is realized between impact and vibratory methods.

Figure A.10 shows the change in shear strength with increasing moisture content for the three compaction methods. The static compaction specimens have consistently lower shear strengths (about 1.2 to 1.4 times) than the impact compaction specimens. Bell (1977) also found that static compaction specimens have lower strength than impact compaction specimens of similar moisture and dry density. Although the mean M_r values for impact and vibratory compaction samples were similar on the dry side of optimum, the τ_{max} of vibratory compaction sample was lower than that of the impact compaction samples.

For all compaction methods, the mean M_r decreased with increasing moisture content with one exception – samples compacted using the static method. The static compaction specimens yielded mean lower M_r (0.7 times) at dry and wet of optimum. The mean M_r for impact and vibratory compaction samples decreased about 1.5 and 2.0 times with increasing moisture from about -3% to +3% of optimum moisture content. The τ_{max} values decreased linearly with increasing moisture content from dry to wet side of optimum for all compaction methods. The static, impact, and vibratory compaction samples showed a trend of decreasing strength (2.4, 3.1, and 2.0 times, respectively), with increasing moisture contents from -3% to +3% of the optimum moisture content.

It should be noted that the trends observed in M_r and τ_{max} with changes in moisture contents are based on one test for each condition. Determining average values with replicate samples at similar conditions may help in better defining the influence of moisture content on these measurements.

Table A.14. Summary of resilient modulus test model coefficients, average M_r, and τ_{max} values for mixed subgrade B material compacted using different compaction methods

Compaction Method	Dry Unit Weight (kN/m^3)	Moisture (%)	Witczak and Uzan (1988) model coefficients				Mean M_r (MPa)	COV (%)	τ_{max} (kPa)
			k_1	k_2	k_3	R^2			
Static	17.34	11.7	679.7	0.38	0.03	0.72	72.5	16.3	269.4
Impact	17.32	11.4	1069.2	0.45	-0.17	0.64	144.8	16.7	373.5
Vibratory	17.41	12.5	1219.7	0.39	-0.08	0.50	148.3	17.7	250.4
Static	17.45	14.3	859.1	-0.01	-0.08	0.10	96.3	21.1	193.3
Impact	17.53	15.2	1011.5	-0.02	-0.21	0.61	130.2	17.3	180.0
Vibratory	17.88	14.2	1571.0	0.54	-0.32	0.77	131.3	31.8	—
Static	17.36	17.2	448.0	0.37	-0.34	0.77	72.1	23.4	110.0
Impact	17.39	17.4	527.7	0.36	-0.22	0.77	74.1	15.2	120.0
Vibratory	17.6	17.1	976.6	0.15	0.04	0.22	96.9	17.6	127.5

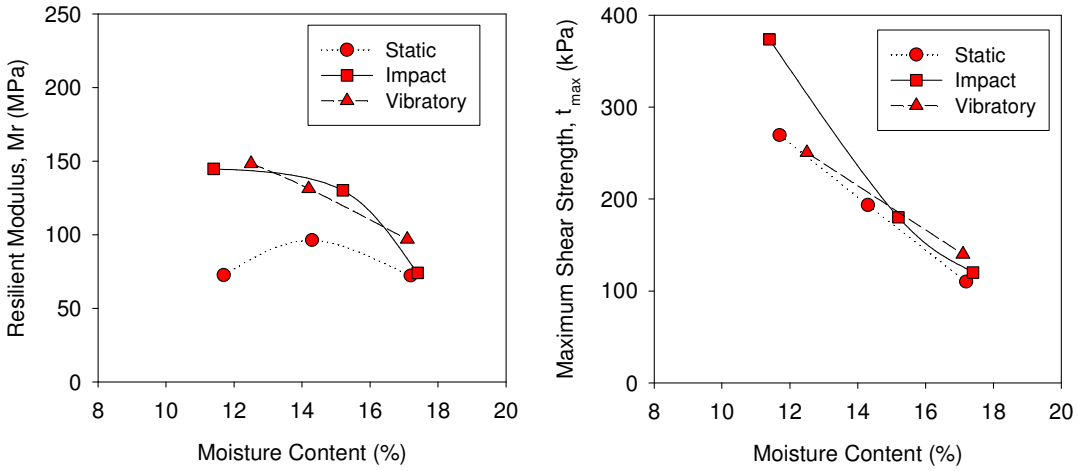

Figure A.10: Influence of compaction method and moisture on (a) mean resilient modulus, and (b) maximum shear strength of mixed subgrade B material

A.8.3.2 Class 5 Base Material

Specimens were compacted at target moisture contents of -3%, 0%, and +3% of optimum moisture content determined by the vibratory compaction test (6.3%) to target dry unit weights. Table A.15 provides summary M_r and UU test results and the constuitive model coefficients (Equation A.1). The mean M_r values and the coefficient of variation (COV) of the value within a test are also shown in Table A.14. Figure A.11a shows the change in mean M_r as a function of moisture content and compaction

method. On average, vibratory compaction samples produced M_r values in the range of about 1.0 to 1.5 times greater than impact compaction samples, with greater differences at optimum and dry of optimum. Figure A.11b shows the change in shear strength with moisture content for different compaction methods. Vibratory compaction samples exhibited τ_{max} of about 1.5 times greater than impact compaction sample at 5.8% moisture content, and no significant differences are realized between the two methods at the other two moisture contents.

Increase in moisture content from 3.6% to 7.7% reduced the mean M_r value by 1.3 and 1.7 times for the impact and vibratory methods, respectively. The shear strength generally decreased with increasing moisture content with one exception, which is observed at 6.1% moisture with impact method. It should be noted that the trends observed in M_r and τ_{max} with changes in moisture contents are based on one test for each condition. Determining average values with replicate samples at similar conditions would help better defining the influence of moisture content on these measurements.

Table A.15. Summary of resilient modulus test model coefficients, average Mr, and τ_{max} values for Class 5 Base material compacted using different compaction methods

Compaction Method	Dry Unit Weight (kN/m^3)	Moisture (%)	Witczak and Uzan (1988) model coefficients				Mean M_r (MPa)	COV (%)	τ_{max} (kPa)
			k_1	k_2	k_3	R^2			
Impact	21.50	3.6	774.5	0.73	-0.15	0.90	180.7	34.6	212.5
Vibratory	21.44	3.8	1255.1	0.63	0.08	0.90	264.1	42.0	188.8
Impact	21.92	5.8	787.1	0.60	0.05	0.96	159.2	37.8	100.6
Vibratory	21.87	6.1	854.3	0.72	0.07	0.94	199.6	51.8	159.6
Impact	21.68	7.6	652.5	0.62	0.15	0.96	135.1	44.4	126.3
Vibratory	21.66	7.7	571.7	0.77	-0.11	0.94	141.7	42.7	137.3

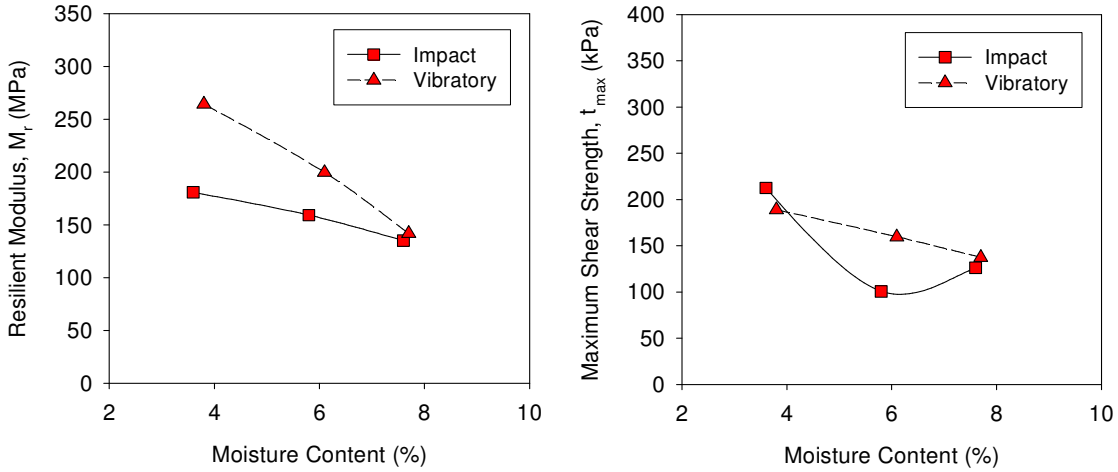

Figure A.11: Influence of compaction method and moisture on (a) mean resilient modulus, and (b) maximum shear strength of class 5 base material

A.8.3.3 Summary of Effects of Compaction Method

The differences in τ_{max} and M_r between the compaction methods are observed for both subgrade and class 5 base materials. In general, the effects appear to be more prominent for cohesive soils, especially when compared between static and impact or vibratory methods. These variations are likely due to variations in the resulting soil structure and potential differences of pore pressures developed during compaction. According to Lambe and Whitman (1969) the compaction method can affect the total stresses and pore pressures within a compacted soil, which affects the strength measurements. Neves (1971) showed that different compaction methods produce distinctly different soil fabric/structure at similar moisture and dry densities. These variations are of consequence as it relates to which lab compaction method is more representative of in-situ soil conditions. Quantifying the effects of soil structure/fabric on soil strength and stiffness properties is complicated. More research is needed to better resolve this issue.

References

Andrei, D., Witczak, M. W., Schwartz, C. W., Uzan, J. (2004). "Harmonized resilient modulus test method for unbound pavement materials." *Journal of Transportation Research Record,* No. 1874, Transportation Research Board, Washington D.C., p. 29–37.

Bell, J. R. (1977). "Compaction energy relationships of cohesive soils." *Transportation Research Record,* No. 641, Transportation Research Board, Washington, D.C., p. 29–34.

Brown, S. F. (1974). "Repeated load testing of a granular material." *Journal of Geotechnical Engineering Division,* ASCE, Vol. 100, No. 7, p. 825 – 841.

Elliott, R. P., and S. Thornton. (1988). "Simplification of subgrade resilient modulus testing", *Transportation Research Record,* No. 1192, Transportation Research Board, Washington, D.C., p. 1–7.

Gabr, M.A., Hopkins, K., Coonse, J., and Hearne, T. (2000). "DCP Criteria for Performance Evaluation of Pavement Layers." *J. Perf. Constr. Fac., Vol.* 14, No. 4, pp. 141-148.

Hicks, R. G. (1970). *Factors influencing the resilient properties of granular materials*. PhD Thesis, University of California at Berkeley, CA.

Hoff, I., Bakløkk, L. J., Aurstad, J. (2004). "Influence of laboratory compaction method on unbound granular materials." *6th International Symposium on Pavements Unbound*, UNBAR 6, Eds. A. R. Dawson, Nottingham, England.

Huang, Y. (1993). *Pavement analysis and design*. Prentice-Hall, Inc.

Kim, W., Labuz, J. (2006). *Resilient modulus and strength of base course with recycled bituminous material.* Final Report submitted to Mn/DOT, University of Minnesota, December.

Lambe, W. T., Whitman, R. V. (1969). *Soil mechanics*. John Wiley and Sons, New York.

Lee, W., Bohra, N. C., Altschaeffl, A. G., White, T. D. (1997). "Resilient modulus of cohesive soils." *Journal of Geotechnical and Geoenvironmental Engineering*, Vol. 123, No. 2. ASCE, p. 131–136.

Livneh, M., Livneh, N. A., and Ishai, I. (2000). "The Israeli experience with the regular and extended dynamic cone penetrometer for pavement and subsoil-strength evaluation." *Proc., Nondestructive Testing of Pavements and Backcalculation of Moduli*, Vol. 3, ASTM STP 1375, S. D. Tayabji and E. O. Lukanen, eds., American Society for Testing and Materials, West Conshohocken, Pa.

Marr, W. A., Hankour, R., Werden, S. (2003). "A fully automated computer controlled resilient modulus testing system", *Resilient Modulus Testing for Pavement Components*, ASTM STP 1437, ASTM International, PA.

McRae, J. L. (1965). *Gyratory testing machine technical manual for bituminous mixtures, soils, and base course materials.* Engineering Developments Company, Inc., Vicksburg, Mississippi, 1965.

Morgan, J. R. (1966). "The response of granular materials to repeated loading", *Proceedings of 3rd Conference of Australian Road Research Board*, p. 1178 – 1192.

Mohammad, L.N., Puppala, A. (1995). "Resilient properties of laboratory compacted subgrade soils." National Academy of Science, *Transportation Research Record,* No. 1504, Transportation Research Board, Washington D.C., p. 87–102.

Monismith, C.L., Hicks, R.G., Salam, Y. (1971). "*Basic properties of pavement components.*" Federal Highway Administration, Berkeley, CA, Final Report FHWA–RD–72–19.

Nazarian S., Yuan D., and Tandon V. (1999). "Structural Field Testing of Flexible Pavement Layers with Seismic Methods for Quality Control." *Transportation Research Record* 1654, pp. 50-60.

Porter, O. J. (1930). *Method of determining relative compaction and shrinkage of soil materials*. Research Department, California Division of Highways.

Ping, W. V., Xing, G., Leonard, M., Yang, Z. (2003). *Evaluation of laboratory compaction techniques for simulating field soil compaction – Phase II.* Research Report No. FL/DOT/RMC/BB – 890 (F), Florida State University, Florida.

Ryden N., and Lowe M. (2004). "Guided wave propagation in three-layer pavement structures." *J Acoust Soc Am,* Vol. 116, No. 5, pp. 2902-2913.

Ryden N., and Park C. B. (2006). "Fast Simulated Annealing Inversion of Surface Waves on Pavements using Phase Velocity Spectra." *Geophysics,* Vol. 71, No. 4, pp. 49-58.

Seed, H. B., Chan, C. K., Lee C. E. (1962). "Resilience characteristics of compacted clays." *Journal of Soil Mechanics and Foundation Engineering,* Vol. 83, No. 4, ASCE, p. 1427–1435.

Smith, D. M. (2000). *Response of granular layers in flexible pavements subjected to aircraft loads.* Ph.D. Dissertation, Louisiana State University, May.

Tanimoto, K., Nishi, M. (1970). "On resilience characteristics of some soils under repeated loading." *Soils and Foundations,* Vol. 10, No. 1, Japan Society of Soil Mechanics and Foundation Engineering, Japan, p. 75–92.

Thompson, M. R., Robnett, Q. L. (1979). "Resilient properties of subgrade soils." *Journal of Transportation Engineering,* Vol. 106, No. 1, ASCE, p. 71–89.

Vennapusa, P., and White, D. J. (2009). "Comparison of light weight deflectometer measurements for pavement foundation materials." *Geotechnical Testing Journal*, Vol. 32, No. 3, pp. 239-251.

Webster, C. R. (1984). *A laboratory investigation of vibratory compaction of dry soils.* M.S. Thesis, Texas A&M University, Texas.

Witczak, M. W., and J. Uzan. (1988). *The Universal Airport Design System, Report I of IV: Granular Material Characterization*. Department of Civil Engineering, University of Maryland, College Park.

Zaman, M., Chen, D-H, Laguros, J, (1994). "Resilient moduli of granular materials*", Journal of Transportation Engineering*, Vol. 120, No. 6, ASCE.

Zeghal, M. (2004). "Discrete-Element Method Investigation of the Resilient Behavior of Granular Materials", *Journal of Transportation Engineering,* ASCE, Vol. 130, No. 4, p. 503 – 509. July.

Zhang, Z., Tao, M., Tumay, M. (2005). "Absorbed energy and compacted cohesive soil performance – Technical Note", *Geotechnical Testing Journal*, Vol. 28, No. 4, ASTM International, PA.